ADDIS ABABA UNIVERSITY
COLLEGE OF NATURAL SCIENCES
SCHOOL OF EARTH SCIENCES

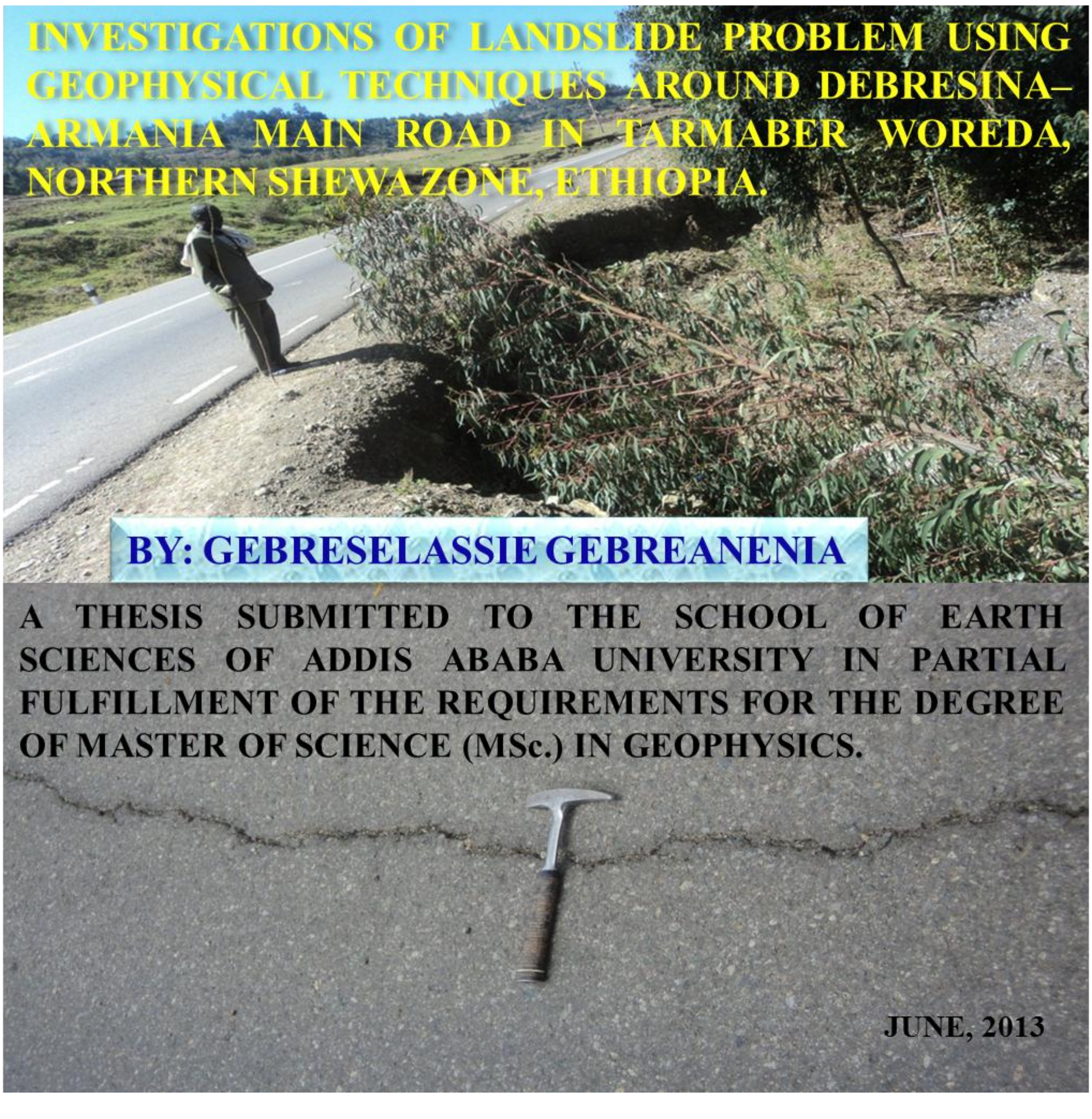

INVESTIGATIONS OF LANDSLIDE PROBLEM USING GEOPHYSICAL TECHNIQUES AROUND DEBRESINA–ARMANIA MAIN ROAD IN TARMABER WOREDA, NORTHERN SHEWA ZONE, ETHIOPIA.

BY: GEBRESELASSIE GEBREANENIA

A THESIS SUBMITTED TO THE SCHOOL OF EARTH SCIENCES OF ADDIS ABABA UNIVERSITY IN PARTIAL FULFILLMENT OF THE REQUIREMENTS FOR THE DEGREE OF MASTER OF SCIENCE (MSc.) IN GEOPHYSICS.

JUNE, 2013

Addis Ababa University
College of Natural Sciences
School of Earth Sciences

INVESTIGATIONS OF LANDSLIDE PROBLEM USING GEOPHYSICAL TECHNIQUES AROUND DEBRESINA–ARMANIA MAIN ROAD IN TARMABER WOREDA, NORTHERN SHEWA ZONE, ETHIOPIA

By: Gebreselassie Gebreanenia

Approved by board of examiners:-

Dr. Seifu Kebede Signature ___________________

Chairman, Department of Earth Science

Dr. Tigstu Haile Signature ___________________

Advisor

Dr. Tilahun Mammo Signature ___________________

Co-Advisor

Dr. Abera Alemu Signature ___________________

Internal Examiner

Dr. Getnet Mewa Signature ___________________

External Examiner

ABSTRACT

Geophysical and geological investigations have been conducted for landslide problem characterization of the existing main road of the study area. The site is located in between Debresina and Armania towns, Tarmaber Woreda, northern Shewa Zone of Amhara Regional State. The main objective of the study was to image subsurface of the problematic main asphalt road, identify triggering mechanisms of landslide problem, and recommend possible mitigation measures based on the geo-electrical resistivity stratification of the site and magnetic anomalies obtained over the survey area. Geophysical investigations using 2D electrical imaging and magnetic methods have been conducted for the landslide problem of the road located at kebele Dokakit near Sar Amba Kidanemhiret locality between Debresina and Armania towns.

From the results of the survey, it has been possible to map the sliding subsurface of the geologic layers, their vertical and lateral extents. It has also been possible to map areas of weakness in the subsurface that could be causing and damaging to the life of the road. According to the interpretation of the geophysical results, the near surface geology of the study area includes fragmented and disturbed layers together with expansive clay soils which have also considerably cause of sliding problem over the area. In profile three the clay soils are much thicker than the other two profiles. In profile three low resistivity deposits are dominant particularly in the northeastern side of the survey area. These deposits are may be huge deposits of the fragmental basalt and expansive clay soils that are moved down the slope and accumulated in location of profile three which is just down the road.

Based on the joint interpretation of the results, the surveyed area has possible slide zone which is characterized by fragmented and structurally disturbed portion which starts from almost half of the surveyed line towards northeast direction. This is interpreted to be the response of the water saturated, weathered and fractured basalt rock. There is also landslide affected subsurface that exhibits intermediate apparent resistivity values comprises of the southwest end of the surveyed profiles. This zone consists of surface of weakness and some displaced rock units.

As conclusion from the work, the asphalt road parallel to the survey profiles has active sliding problem and cracks especially at the two ends of the profiles. The different weak zones, deeply weathering conditions, action of rain fall, springs and slope nature of the study area were the causing factors for this sliding problem. Therefore, special attention should be given to maintain and protect from further sliding problem.

ACKNOWLEDGEMENT

Above all, I would like to thank "Almighty God" who made it possible to begin and finish this work successfully. Next, it gives me a pleasure to thank all individuals and organizations who contributed to the success of this work.

First and foremost I am grateful to my advisors Dr.Tigistu Haile and Dr. Tilahun Mammo for their help during data processes, fatherly approaches, encouragements, constructive comments and suggestions throughout the research work. Thank you very much Dr.Tigistu for your unforgettable help you did during all the ups and downs of my field work.

My warmest gratitude goes to the Ethiopian Road Authority for allowing me car during my field work in the Debresina area. It was difficult to complete my field work without their help. I also thank for Ethiopian Institute of Geological Survey for the reference materials they gave me during my data collection and Ethiopian Meteorology Agency for their permission to use the rainfall data of the area.

Special appreciations go to Dr. Asmelash Abay, Prof. Gezahegn Yirgu, Dr.Tarun K.Raghuvanshi for their help in various geological and landslide explanations of the study area.

It gives me a special privilege to extend my deep thanks to my friends Hailemariam Siyum, Tesfay Kiros, Mohammed Yosuf, Alemayoh Ayele and others for their support and comments that they gave me during my research work.

Last but not least, I sincerely thank to all my beloved family for their love and encouragement. I do not have words to thank particularly my sister Helen for her treatments and bases for my success.

Contents **Pages**

List of Figures

List of Tables

List of Annexes

Acronyms

2D	Two Dimensional
DEM	Digital Elevation Model
EIGS	Ethiopian Institute of Geological Survey
EMA	Ethiopian Meteorology Agency
ERA	Ethiopian Road Authority
ERT	Electrical Resistivity Tomography
GIS	Geographical Information System
GPS	Global Positioning System
GTP	Growth and Transformation Plan
IGRF	International Geomagnetic Reference Field
MER	Main Ethiopian Rift
NE	Northeast
SW	Southwest
RMS	Root Mean Square Error
RTP	Reduction to the Pole
UTM	Universal Transversal Mercator
VES	Vertical Electrical Sounding

CHAPTER – ONE

1. INTRODUCTION

1.1 General

Landslides are one of the major destructive natural hazards and have been affected human lives, infrastructures, agricultural lands and natural environment in various parts of the highlands and rift margins of Ethiopia (Lulseged Ayalew, 1999; Temesgen, et al, 2001; Lulseged Ayalew and H. Yamagishi, 2004; Tenalem Ayenew and Barbieri G., 2005; Kifle Woldearegay, 2005) as cited in Asmelash Abay (2012). In the years 1990-1998 alone, landslides or landslide-generated hazards have claimed about 300 human lives, damaged over 100 km asphalt road, demolished more than 200 dwelling houses and devastated in excess of 500 hectares of land in different areas of the highlands of Ethiopia (Lulseged Ayalew, 1999) as cited in Asmelash Abay (2012).

Some of the main roads of the country like Goha Tsion-Dejen road of the Abay gorge; Debresina-Armania; Kombelcha-Dessie; wuchale-Wurgessa-Mersa; Alamata-Korem-Maichew-Alaje; Adigrat-Mugulat-Bizet and some other areas have been threatened by the slope failures when crossing the landslide susceptible landscapes of the rift margins (Asmelash Abay, 2012).

The Debresina area is one of the most landslide prone areas of Ethiopia and is located in the Afar Rift Margin. The main road of the study area is located between Debresina-Armania towns and one of the landslide affected sections of the Addis Ababa-Dessie-Mekelle main asphalted road. Many cracks and landslide caused problems are observed at the main road of Debresina-Armania towns. To protect the loss of lives and cost suffered from landslide incidences, it is useful to understand the causes and characteristics of the landslide processes; determine the extent of the slope instabilities and carry out appropriate mitigation measures. Therefore, this study was designed to understand the subsurface conditions of the problematic section of the main asphalt road between Debresina and Armania with a view to; identifying the triggering mechanisms of the landslide problem, and recommend possible mitigation measures.

1.2 Statement of the problem

Nowadays, Ethiopia has many existing and under construction main roads which are used to connect different parts of the country and the country to the neighboring countries. The five year goals of Growth and Transformation Plan (GTP) of Ethiopia include construction of roads even through different villages because these roads are believed to have a major contribution to the development of the country.

Problem of landslide has been the major threat to people, property and the natural or built environment such as roads, houses, farmlands, etc. Some of the roads of the country have been damaged by landslide problem and this may cause loss of lives, vehicles and inhibiting traffic between towns. Thus, road failure due to landslide problem can also cause severe hardship for those dependent on it for their livelihood by upsetting the regular transport condition of the main road.

Landslide is the main problem through the asphaltic road of Addis Ababa-Mekelle towns because the road of the study area has been the main vein that connects Addis Ababa with many towns of northern Ethiopia. It is also located at an area highly susceptible to landslide and a large part of the main road is endangered with this problem (Figure 1.1). Many researchers have visited the study area and it's surrounding for different purposes but there was no particular works along the main road by proposed geophysical investigation for the landslide problem investigations of the study area. Therefore, this research was conducted to identify the major causes and to recommend possible remedial countermeasures of landslide around the Debresina–Armania asphalt road of the Tarmaber Wereda.

Figure 1.1 Slides showing views of landslide effects at the main asphalt road of the site.

1.3 Description of the Study Area

1.3.1 Location and accessibility

The study area is located between the towns of Debre Sina and Armania, Tarmaber Woreda, northern Shewa Zone of Amhara Regional State (Figure 1.2). It is at about 200 km NE of Addis Ababa. The study area is accessible through the Addis Ababa-Dessie asphaltic road. Planned geological traverses were accomplished by foot trails across the ups and downs of the rugged topography of the study area but the geophysical surveys are conducted on the sides of the main asphaltic road and areas adjoining it. The study area is bounded by geographic UTM coordinates of 586000-591000m E and 1088000-1093000m N. The total study area covers an area of 24.78 km^2.

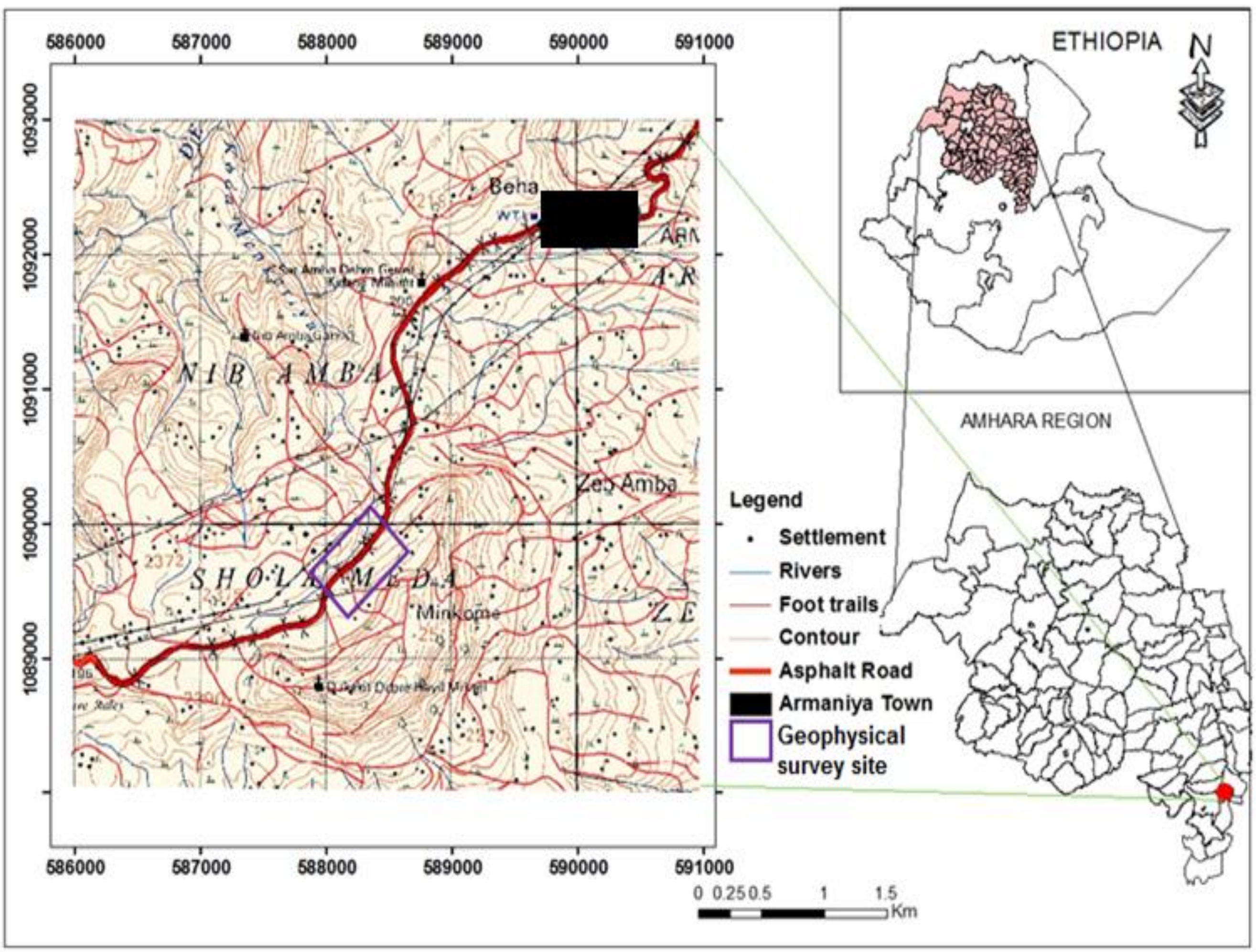

Figure 1.2 Location map of the study area.

1.3.2 Climatic conditions of the study area.

The climate of Ethiopia is generally characterized by different seasons. However, for the interpretation of the climatic condition in the study area, data from National Meteorological Service Agency of Ethiopia, at Debresina station, was referred for thirty three years (1980-2012) and the study area is characterized by "Weyna dega" climatic zone.

The study area is mainly known by wet and cold climate and rarely the temperature reaches below 0^{0}C. During winter it has cold and humid climate, whereas relatively hot and dry climate in summer. Two main rainy seasons in the region are Belg (mid-February to mid-March) and Kiremte (mid-June to mid-Sept) with moderate and high precipitation, respectively. Monitoring the variability of climate that is responsible for the coming effect on an area needs the knowledge of the climatology of that area. This means knowing the long-term mean values of climatic parameters such as temperature, rainfall, etc. and their degree of variability or deviation from the mean is very important.

1.3.3 Physiography of the study area

The study area is part of the central western Ethiopian plateau. It also occupies the southwestern margin of the Afar Rift system represented by very rugged topography as a result of rift forming tectonics. In the map of the area, there is a considerable difference in altitude ranging from 1800 m to 2600m above sea level. The topographic surface of the area is irregular, with many cliffs alternating with steep and gentle slopes, valleys and flat lying surface. The high altitude ridges and related steep escarpments physiographic region generally occupy the western and southern part, which consists of the highest elevation of the area. It is characterized by highly elevated and N-S trending ridges as well as mountain chains, which form steep escarpments. The main road passes through the mountainous topography which is bounded by cliff land on the eastern side and a relatively gentle slope on the western side.

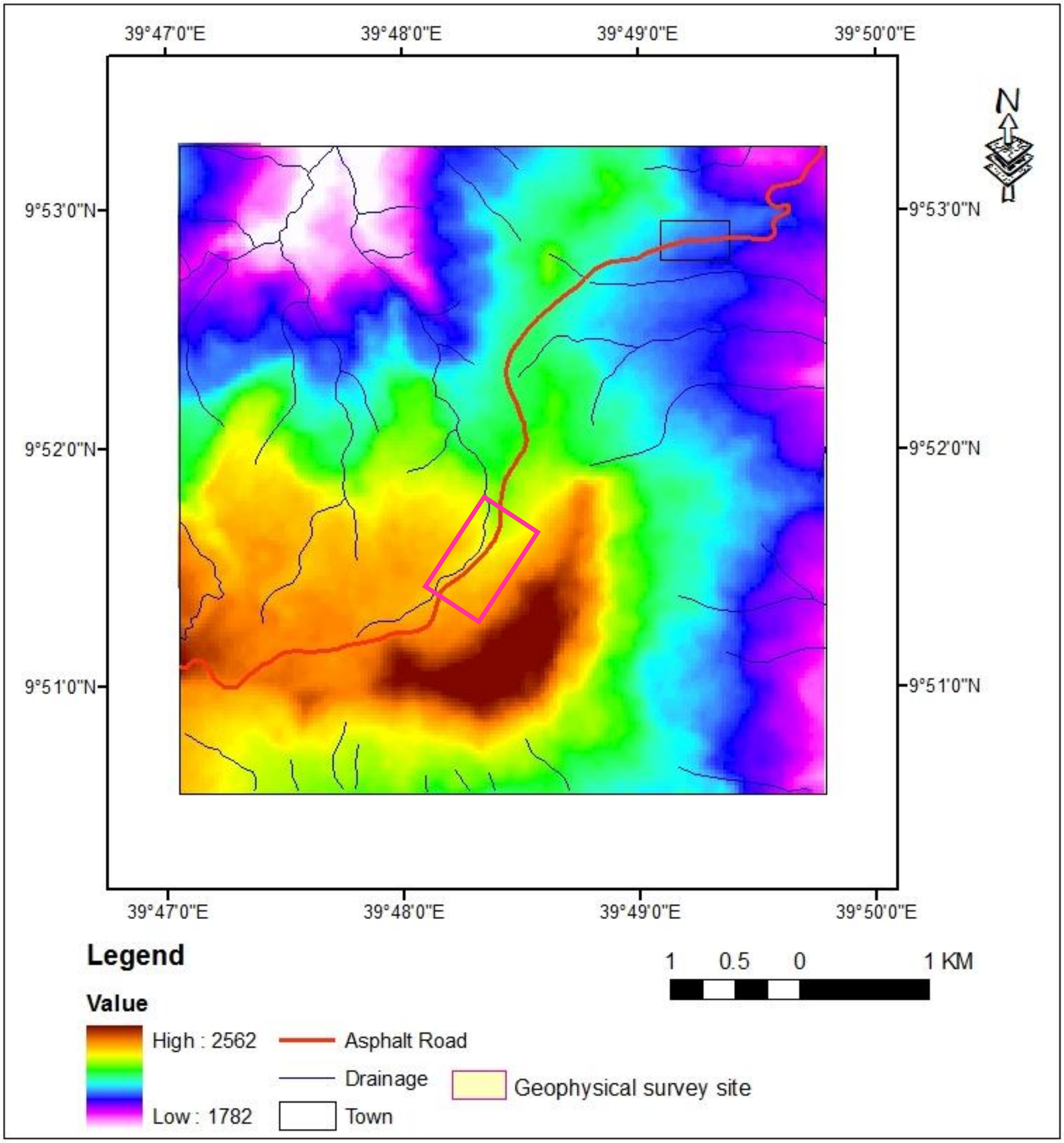

Figure 1.3 Digital Elevation Model (DEM) of the study area

1.3.4 Seismicity of the study area

The important steps in assessment of seismicity are identifying the seismic source zones, distance to the site and geology of the site. In this respect, the study area is located in the south western margin of Afar rift system which is tectonically active. The geology of the project site is covered by recent loose sediments. The sediments and faults have an ability to amplify the amplitude of the seismic waves. Because of these reasons even small magnitude of earthquake might damage the structures easily.

Plainly speaking, with the present static knowledge, earthquakes can never be predicted accurately and hence to develop a system of warning and eliminating the risk of loss to life is yet a distance dream (Singh, 1997). However, structures in many earthquake prone countries are now being designed more safely from information obtained from seismic zonation maps of this type.

According to the Ethiopia Building Code Standard (1995), the country is divided into five zones approximately equal seismic risks depending on the known distribution of earthquakes. These zones are no damaging zone (0 zones), less damaging zones (zones 1 and 2) and zones of major damaging (zones 3 and 4). From the seismic hazard map of Ethiopia, the project site is located at the boundary of zone four and very near to zone three as shown in Figure 1.4. This map is based on the amplitudes of the ground acceleration to be expected during 100 years return period. According to the building code, the ground acceleration ratio (αo) depends on the seismic zones.

Table 1.1 Bedrock acceleration ratio

Zone	4	3	2	1
α^{o}	0.10	0.07	0.05	0.03

The ground acceleration value of the project site is 0.10g for 100 year return period. Therefore, design of any infrastructures at the study area should include all necessary seismic resistant design parameters.

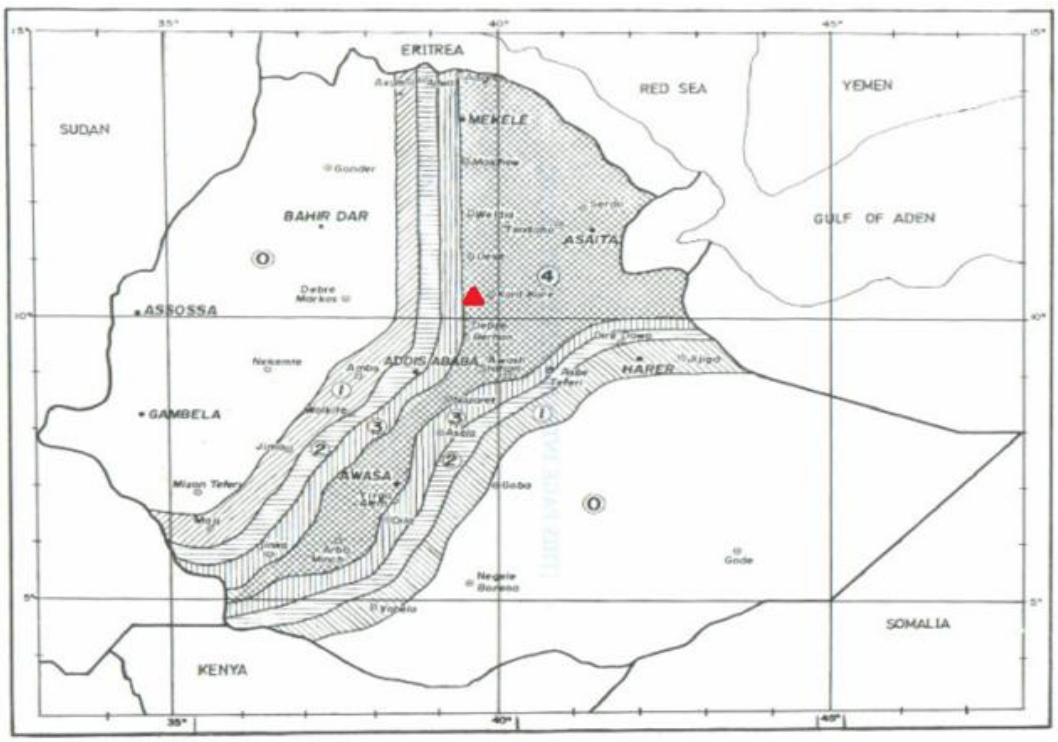

Figure 1.4 Seismic hazards zoning of Ethiopia (Ethiopian Building Code standards, 1995) and location of the study area (shaded triangle).

1.4 Objectives of the study

1.4.1 General objective

This research was conducted to study the subsurface conditions of the problematic section of the main asphalt road between Debresina and Armania with a view to; identifying the triggering mechanisms of the landslide problem, and recommend possible mitigation measures.

1.4.2 Specific objectives

The specific objectives of the research include:

- Mapping of geological lithologies around the problematic section of the main asphalt road of the area.
- Identifying of anomalous geological conditions like lithological contacts and structures those contribute to landslide occurrence over the area.
- Assessing of the extent of landslide problems in the section of the investigated area.

1.5 Methodology

In order to achieve the objectives of the study formulated in section 1.4 various stages and techniques of data collection were employed. Literature on geophysical investigation techniques as applied to landslide studies were thoroughly reviewed. For this, different textbooks, journals, various official documents, published and unpublished papers from various professionals on geophysical investigations for landslide problem characterization were reviewed. But, primary data pertaining to the present research work of the study area were collected from the field activities during the reconnaissance and main field works. The relevant secondary data were also collected from respective offices like Ethiopian Road Authority (ERA), Ethiopian Institute of Geological Survey (EIGS), and Ethiopian Meteorology Agency (EMA). The major lithologies and geological structures were mapped following survey traverses.

The geophysical investigations were conducted using the techniques of Electrical Resistivity Tomography (ERT) and Magnetic Survey. Data were collected along selected profiles and over random points (especially for magnetic method) well distributed to cover the investigation site. The spatial geophysical mapping, modeling and interpretation has been assisted using appropriate software such as the ElectreII, ProsysII, RES2DINV, Geosoft Oasis Montaj 6.4.2, Microsoft Excel and Surfer 9.11. The geological map and geological crossections were also developed using ArcGIS 9.3, Global Mapper 11, and 3DEM softwares.

Accordingly maps and models were produced and interpreted to obtain information required to meet the tasks set out in the research objectives. The generalized flow chart of methodological approach that was used for this investigation is given in Figure 1.5.

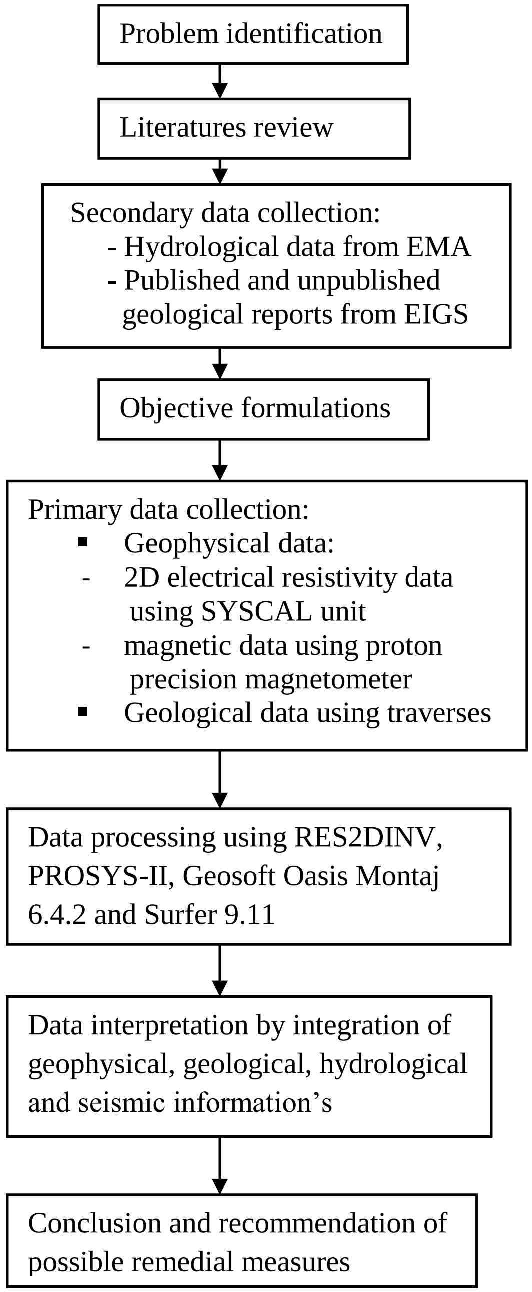

Figure 1.5 Flow chart of the methodologies applied for this research work investigation.

1.6 Previous studies in and around the study area

The following are some of the works in different landslide susceptible areas of Ethiopia:

Solomon Gerra (2010) has conducted integrated landslide investigations in Tarmaber and surroundings which is in the northwestern side of the study area. Based on this work, integrated geological, engineering geological, hydrogeological and geophysical investigations were carried out. Geophysical studies were also carrying out from April to May 2010 in the project area at five selected sites, namely, Kechine, Barmeda, Babota, Yebegoch-Gat and Yemariam-Wonz. Among the methods, Vertical Electrical Sounding (VES), magnetic and Seismic Refraction were implemented.

Engineering geophysical investigation along a proposed alternative route of Blue Nile Gorge has been conducted (EIGS, 1994). The survey methods used were refraction seismic, electrical resistivity (VES and profiling) and magnetic with the objectives of determining depth to the bed rock, locating possible structural features, and studying the nature of the overburden material.

The integrated engineering geological and geophysical investigations for landslide studies in Bonga town and its surroundings have been conducted (EIGS, 1999). The geophysical methods, which consisted of Refraction seismic, Vertical Electrical Sounding, Electrical resistivity profiling and magnetics, were conducted along 27 profiles covering a total length of 7.6 km.

Many researchers have visited the study area and it's surrounding for different purposes but there was no particular works along the main road by proposed geophysical methods for the landslide problem investigations of the study area. A number of works have been done by different scholars. Some of the relevant works are:

Asmelash Abay and Giulio Barbieri (2012) have conducted investigation landslide susceptibility and causative factors evaluation of the landslide area of Debresina, in the Southwestern Afar Escarpment, Ethiopia. Based on this work, the landslide susceptibility areas and different causative factors are outlined.

According to Mengesha et al., (1996), the olivine basalt of Debresina belongs to the Tertiary volcanism. This rock came out as lava flows through tectonic fractures and fault planes related to the great rift valley of East Africa.

Zanittine et al., 1974, noted that the ignimbrites of the Debre Berhan and Tarmaber area are covered by Tarmaber Basalt. In this work, K/Ar age determinations gave values of 15.4+/-0.3 Ma for the upper member of the ignimbrite sequence and 13+/-0.6 Ma for the overlaying basaltic flows.

Alula and Gashawbeza (1993) have conducted investigation for coal and oil shale on 145 sq km area located 30 km north of Debre Berhan. Accordingly, basalts, ignimbrites and inter-volcanic sediment, which contain carbonaceous shale and coal seams, are reported. Mengesha et al, (1996) in the 1:2, 000, 000 scale geological map of Ethiopia has described that the map area is covered by rhyolites, trachyte and transitional to sub-alkaline basalts of Alaji Formation as well as by transitional and alkaline basalts of Tarmaber-Megezez Formation.

Yonas and Matebie (2006) have mapped the entire project area and produced 1:50, 000 scale geological maps as well as accompanied report. Based on this work, the area is covered by various types of basalts, rhyolites, ignimbrites as well as by inter-volcanic sediments.

Leta Alemayehu (2007) has conducted landslide susceptibility modeling using logistic regression and artificial neural networks in GIS. Based on this work, the landslide zoning and slope instability problem of the selected area has been assessed using remote sensing technique and GIS.

CHAPTER - TWO

GEOLOGICAL, HYDROGEOLOGICAL AND LANDSLIDE INVESTIGATIONS IN THE STUDY AREA

2.1 Geological Investigations of the study area

2.1.1 Regional Geology

Tertiary volcanic rock of central Ethiopia plateau consists of Aiba basalt, Alagi rhyolites and basalts, Tarmaber basalt and Balchi rhyolites (Zanettine, 1974). The Alagi series contain interbeded layers of rhyolites and basalts with an age range of 32 to16 Ma. (Oligocene-Miocene) overlying the Aiba basalts (34-28 Ma; Middle -Upper Oligocene).

The Alagi rhyolites are first silicic rocks emitted in the central eastern Ethiopia plateau making up large ignimbrite unit lying directly on the Aiba basalts or inter-layered in varying quantities with the Alagi basalts (Zanettine et al., 1974). The Aiba basalt is a thick cover of flood basalts out poured on the Ashangi peneplain as a result of distensile crustal movement. The Tarmaber basalt that covers the Oligocene Alagi is termed as Tarmaber Meghezez basalt (Late Miocene). Except Tarmaber basalts, the Alagi volcanics and the Aiba basalts are formed by fissural type of volcanism.

2.1.2 Local Geology

2.1.2.1 Introduction

The study area has different tertiary volcanic rocks and quaternary sediments and these different units are briefly described below.

2.1.2.1.1 Aphanitic basalt

This rock unit crops out in the north western, western and eastern part of the study area. It also outcrops in the continuous cliff forming escarpments. It is characterized by moderately to steep cliff forming topography, which directly overlies the underlying pyroclastic rocks. Its thickness increases from central to western part and attains a maximum of 250 m.

The rock has pinkish gray in weather color, dark gray in fresh color, fine grained texture volcanic rock. It appears massive but it is highly weathering due to jointing and fracturing. It is characterized by different secondary structures like fractures, joints and shear zones (Figure 2.1). They are more intense as one goes from the central to the western part.

Figure 2.1 Fractured and weathered aphanitic basalt rock exposed at northeastern side of the area.

2.1.2.1.2 Vesicular basalt

It is exposed in the northern and western part of the study area. In the western side of the study area it is massive but in the northern part it is highly weathered and jointed rock unit. This weathering becomes very intense at the base where the rock is entirely changed to soil. The unit is columnarily jointed and rock falls are associated with these columnar joint. The rock has light gray weathered, dark gray fresh colored and fine to medium grained rock (Figure 2.2). It shows rounded to sub-rounded vesicles whose max size reaches up to 8 cm. Vesicles are filled-up by greenish and reddish brown secondary minerals, which could be zeolite and hematite, respectively.

Figure 2.2 Jointed vesicular basalt rock at central part of the study area.

2.1.2.1.3 Ignimbrite

It is moderately to strongly stratified, often massive looking rock. Outcrops are always interlayered with the basalt and are exposed at various horizons. At different locations, this rock type has variable thicknesses. The lowest and highest thicknesses are observed in the western part, whereas in the central and southern part it is moderately thick. In the western part the thickness of this rock ranges up to 20 m, whereas in the southern part reaches up to 7m. It has yellowish gray weathered, light gray fresh colored and fine to medium grained rock unit (Figure 2.3). In western part of the study area it is strongly compacted but it highly jointed and weathered in the northern part. The fiamme and lithic fragments contained in this rock are highly aligned parallel to the plane of stratification.

Figure 2.3 Fractured ignimbrite rocks located in between Sar Amba and Armania small towns.

2.1.2.1.4 Interlayered aphanitic basalt, rhyolite and ignimbrite rocks

This unit conformably overlies the underlying basaltic rock and crops out in the western part of the study area at UTM location of 587236E and 1091497N. The thickness of this rock unit approximately reaches up to 90m. The rhyolite and ignimbrite are closely interlayered each other whereas the basalt usually caped the two rocks. Detail description is presented below (Figure 2.4).

Rhyolite: it is layered and massive looking, brownish weathered and light gray fresh color and fine to medium grained rock. Joints as well as fractures are also present on this rock. Thickness of this rock was approximately reaches of 25m meters. This rock is inconsistently weathered and the weathered surface shows yellowish gray, brownish gray and dark gray color.

Ignimbrite: it is light gray to dark gray colored, fine to medium grained, highly compacted as well as well stratified rock. Often, it is subjected to two sets of joints; which are systematic and random type of joints. Its thickness approximately reaches up to 20m. The ignimbrite characteristically consists of fiamme, which is highly elliptical and aligned parallel to the stratification.

Aphanitic basalt: it is moderately to highly weathered stratifying rock. Layering is commonly sub-horizontal. The lowest and highest thicknesses are observed in the top and bottom part this lithological succession which is 15m and 30m thick respectively. Joints and fractures are observed in this type of rock. It has dark gray to bluish gray color, and fine grained texture.

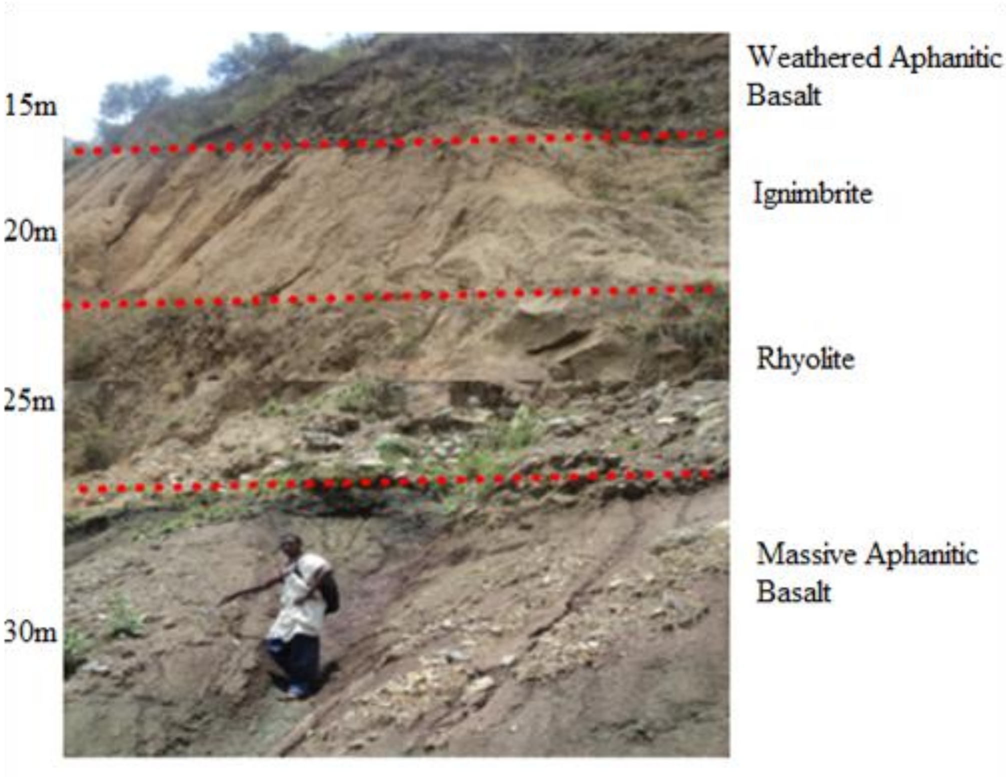

Figure 2.4 Lithological intercalations at western side of the study area (587236E, 1091497N).

2.1.2.1.5 Tuff

This pyroclastic unit is exposed at western and north western portion of the study area. It is characterized by whitish color and fine-grained texture (Figure 2.5). The tuff unit of the study area is relatively light in weight.

Figure 2.5 Tuff rock units at western side of the study area.

2.1.2.1.6 Quaternary sediments

These were exposed at the central, northwestern and northeastern part of the study area. These sediments were composed of cobbles, sands, silt and clay sized soil particles derived by weathering and erosion of different rocks. These deposits were mostly thick residual deposits and there were also some deposits of colluvium-eluvium and alluvial soil deposits in northwestern, eastern and northern part of the study area. The residual soils have formed from insitu weathering of parent materials. In western side of the study area colluvial soils are deposits that displaced from their original location of formation by gravity forces. It was easily observed from river and road cuts; the thickness of these deposits was ranged from 2m up to 20m throughout the study area.

Figure 2.6 Residual clay soils at Shola Wuha locality of the study area showing the deep near vertical fissures.

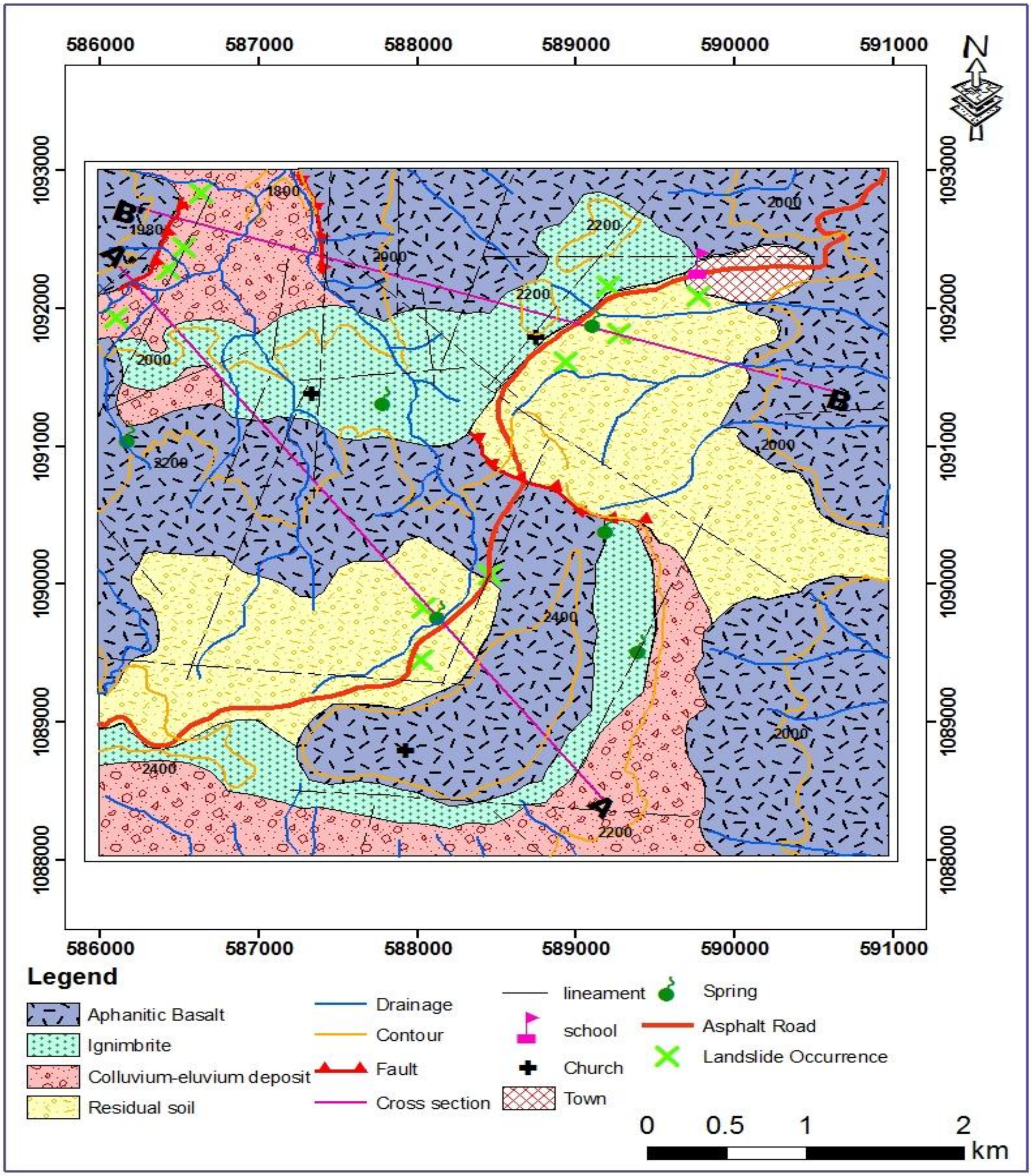

Figure 2.7 Geological map of the study area.

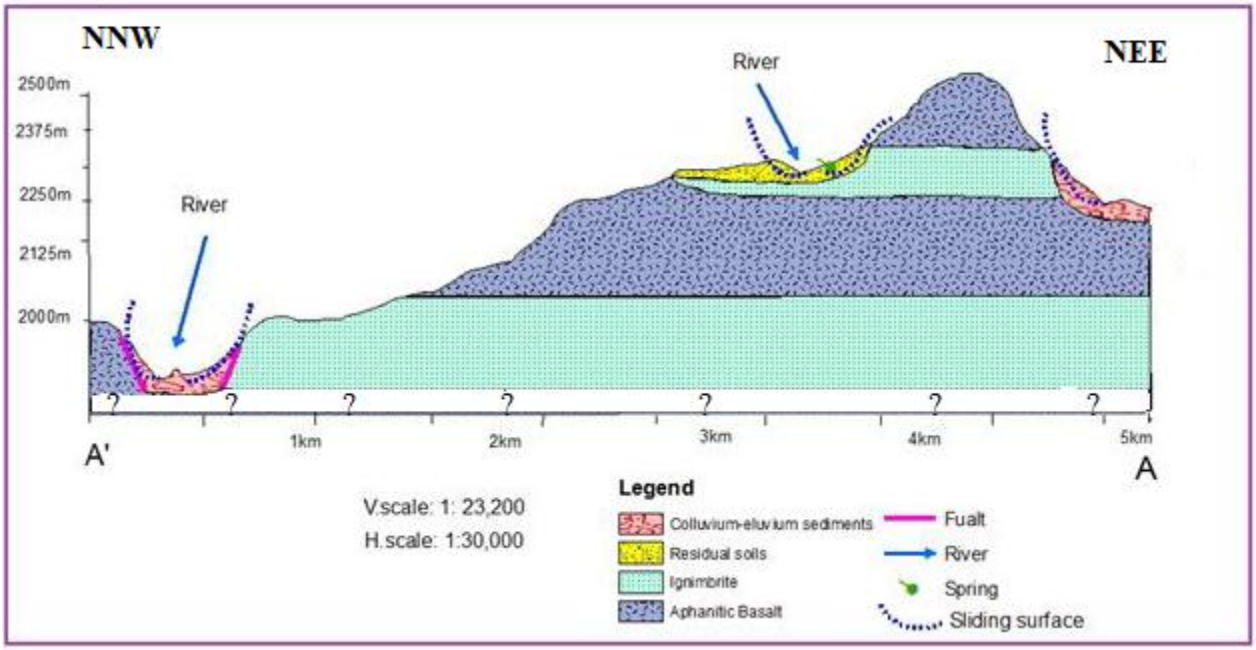

Figure 2.8 Geological cross-section along line A-A'

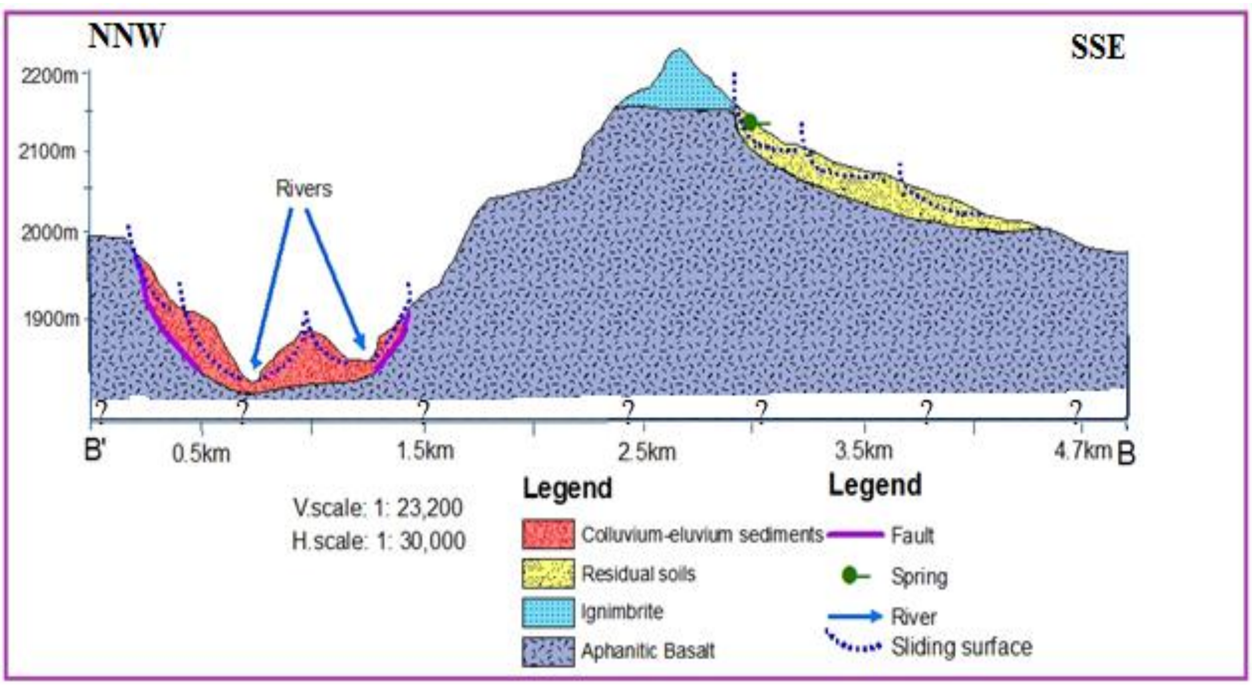

Figure 2.9 Geological cross-section along line B-B'

2.1.3 Local geological structures

In the project area, various structures such as joints, fractures, stratifications, lineaments as well as faults are observed.

2.1.3.1 Joints

The most commonly joint types observed in the study area are columnar joints (Figure 2.10) and normal systematic joints which were 30cm spaced and 20cm aperture. They can be one factor for the sliding problem of the study area.

Figure 2.10 Columnar joints observed in vesicular basalt at location of (588301E and 1091179N).

2.1.3.2 Faults

These structures are observed specially in the western part of the study area. The normal faults are megascopic structures, which have characteristically NNE-SSW and are parallel to the MER trend. They are discontinuous boundary faults that give rise to major fault-escarpments separating the rift depression from the Ethiopian plateau. These faults are normally long, widely spaced and are characterized by large vertical offsets (Figure 2.11).

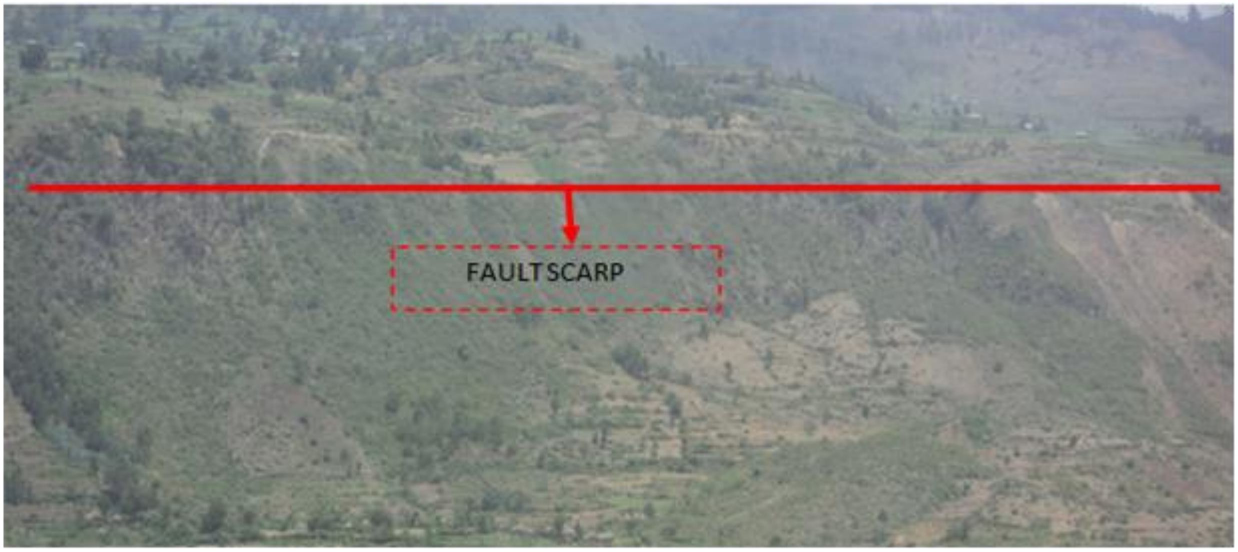

Figure 2.11 Fault escarpments at the western side of the study area.

2.1.3.3 Dykes

There are number of basaltic dykes with strike orientation of NW-SE exposed at southern side of the study area (Figure 2.12). These dykes have an average width of 1 to 2 meters. These are weak zones which were used as channel of basaltic lavas flows to the surface.

Figure 2.12 Dykes at the southern side of the study area (587578E, 1088507N).

2.2 Hydrogeological investigations of the study area

Hydrogeology plays a major role in controlling the occurrence of landslide in the study area. However, there are no boreholes data and other relevant studies that indicate the ground water level of the study area. Therefore, the hydrogeology was discussed based on the field observation of perennial streams and a number of springs of the study area.

2.2.1 Rainfall

Rainfall is one of the most important factors in triggering landslide conditions. The rainfall of the study area is characterized mostly by one long rainy season that last from June to September. The data measure at Debresina rain gauge station indicates the maximum annual rainfall was 727.2mm which was recorded in August, 1997; while the minimum was 0mm almost in most of the years starting from October up to February. The highest average monthly rainfall was also 432.65mm which was recorded in the month of August. The highest average annual rainfall was 201.8mm and recorded at the year of 1998 over the past 33 years recorded data at Debresina station (Annex-I). The sliding problem of the study area particularly at the main road was happened following intense rainy seasons.

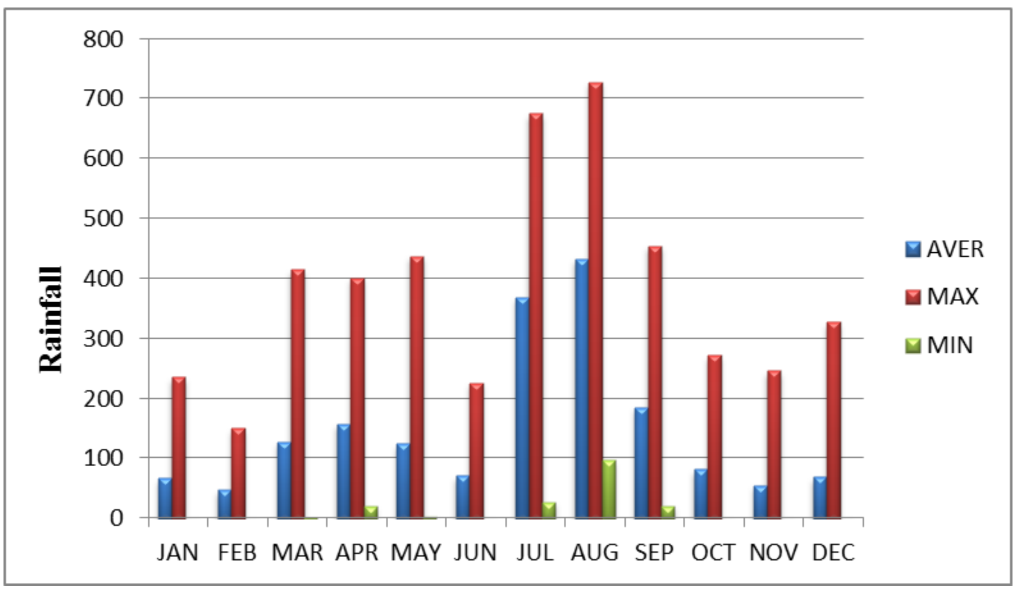

Figure 2.13 Bar graphs showing average, maximum and minimum monthly rainfall of the last 33 years at Debresina station (1980-2012).

2.2.2 Springs

The springs in study area have high discharge and many distributions. During the field work six springs were inventoried in the study area. The two springs are along the down road of the study area which have significant role in landslide of the main road. The observed springs were generally slope control and perennial; increase their yields drastically from dry to rainy season. They flow out in significant amount and can carry huge amount of debris. The springs are functionally helpful for water supply and other domestic purpose (Table 2.1).

Table 2.1Inventories of springs in the study area

Number of springs	UTM location		Elevation(m)	Mode of occurrence	Local place	Their important
	X	Y				
1	588199	1089672	2297	Slope control down the road	Shola Wuha	Free flow
2	589202	1090405	2216	structural control	Ayalfush	Water supply for Chira meda and Armaniya
3	586170	1091061	2074	Slope control	Alihudade	Water supply for local peoples
4	587790	1091340	2051	Slope control	Abil Amba	Water supply for local peoples
5	589120	1091906	2122	Slope control down the road	biera	Water supply for local peoples
6	589402	1089550	2224	Slope control	Zeb Amba	Free flow

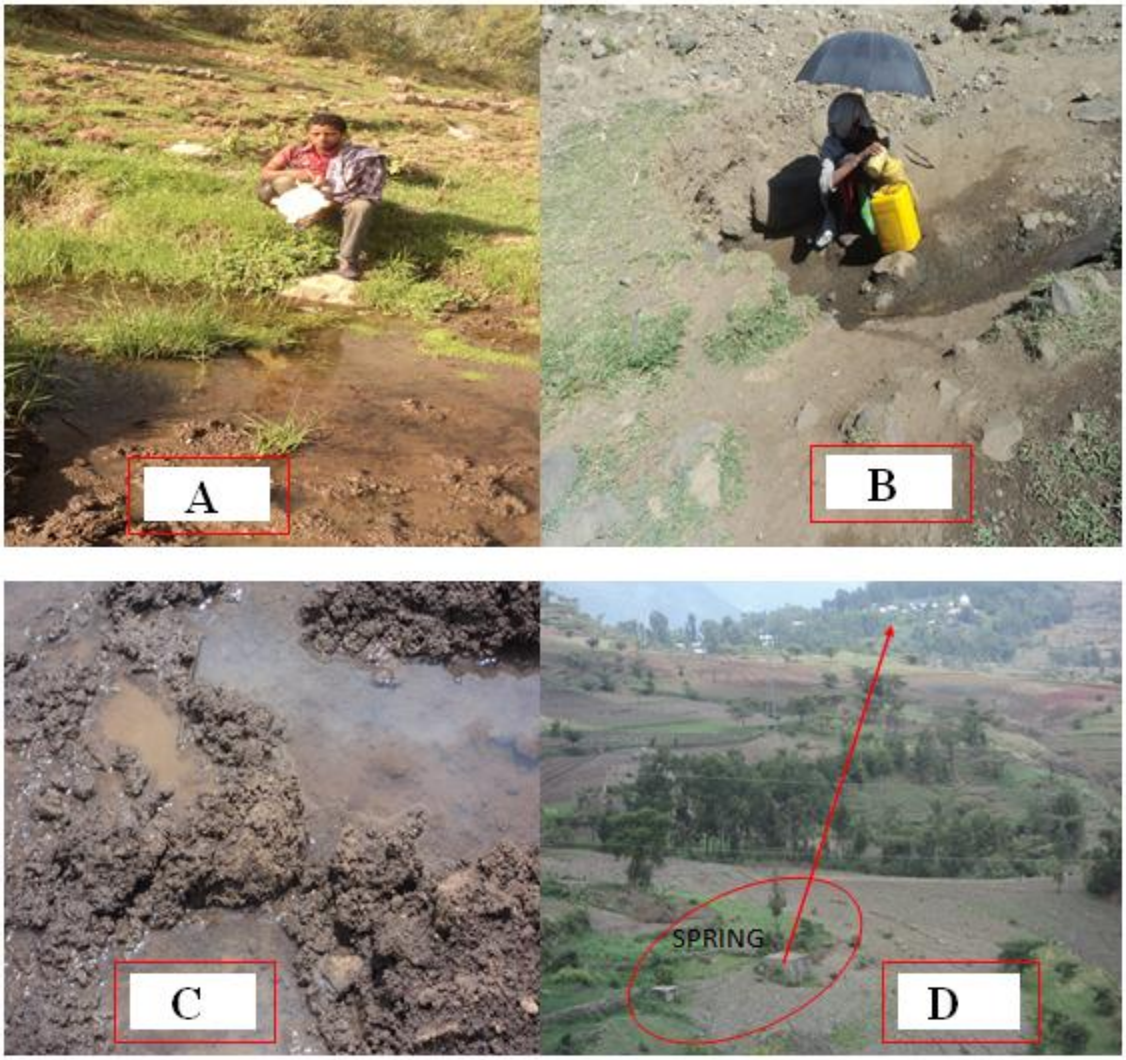

Figure 2.14 Photos showing some of the springs and seepage in the study area: (a) seepage from down the road of Dokakit kebele; (b) spring from down the road of Tikur Chicka locality; (c) seepage from the mountain of Zeb Amba at eastern side of the study area; (d) spring at Ayalfush locality that was used as water supply for Armaniya and Chira Meda towns.

2.2.3 Surface water of the area

There are a number of perennial streams flowing out from the study area. In the northeastern side of the study area which is around Armania town, all the streams are flowing into Meka Main River. From field observation, these rivers have significant role in inducing landslide problem at the section of the main road and its localities.

The other rivers namely Koda Menkeriya, Nech Amba and Teter are found in northwest direction of the study area. They flow out from the area into Dem Aytemashy Main River. This locality also affected by sliding problem following the direction those streams.

All the streams found in southern side of the study area are also flowing out towards the Shenkorge main river. Generally, all these streams, springs and rainfalls have important role in inducing landslide problems.

2.3 Landslide investigations of the study area

The study area is characterized by different types of landslides but the abundant occurrences are rotational types. These rotational landslides are located especially at southern, western and northeastern direction of the study area.

2.3.1 Types of landslide in the study area

2.3.1.1 Rock slide

These are occurred mostly at the road cut of northeast of the study area. They are observed on slopes where competent and relatively less competent rocks are in contact (Figure 2.15). They vary in size from very small to large blocks of rocks.

Figure 2.15 Rock slides at main road of study area

2.3.1.2 Rock falling

The study area consists of individual rock blocks that detached from a steep slope and descending by falling or rolling and coming to rest on gentler slopes in the area. Where these occur frequently, the bedrock is usually moderately to highly fracture with parallel and intersecting discontinuities with slopes. The falling of rocks varies in size mostly as a single rock, single block, mass of blocks and often occurs rapidly without warning. The whole main asphalt road of the study area has rock falling problem and the drainage system is disturbed by this kind of problem (Figure 2.16).

Figure 2.16 Rock falls at main road of study area

2.3.1.3 Rotational slides

These slides in the area are common at steep slopes especially during the periods of intense rainfall. They tend to be deep failures and occur along planes of weakness between overlying colluvial soils and highly weathered rocks. Recently, these have started at gentle slopes of the main road. Rotational slides are usually where sliding material moves along a curved surface and develop from tension scars in the upper part of a slope (Figure 2.17).

Figure 2.17 Tensional cracks down the road at Shola Wuha locality

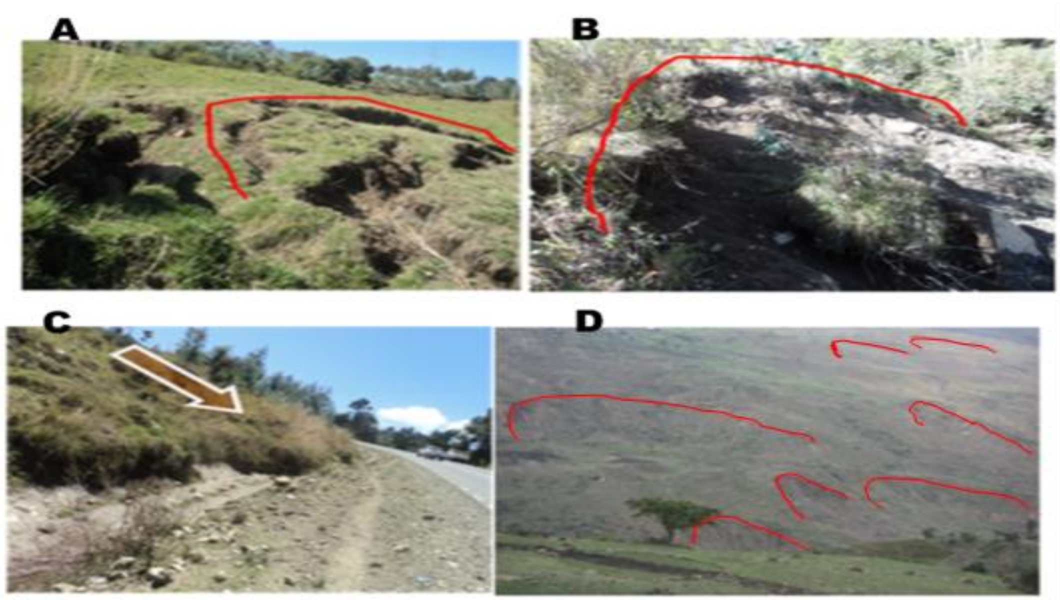

Figure 2.18 Different types of rotational landslide: A&B are slides down the road at Shola Wuha locality; C) slide occurred above the main road at Shola Wuha locality and D) many rotational slides at northwestern near Shotel Amba locality.

2.3.2 The causes of landslide in the study area

From the field observations, the sliding problem in the area is due to the highly weathered geological lithologies, topography, hydrology and human activities which are some of the most important factors that have caused landslides in the study area. Deforestation for housing, agricultural activities, search for building material and road construction have generally assumed to be the preconditioning agents of slope failure in the area. Based on the all rounded information and interpretations the major factors which influence the slope stability are described below.

2.3.2.1 Geological causes

The geological rocks in the study area were highly affected by intense and deep weathering conditions and this considered as one of the main cause for landslide problem. Thus, the lithological map of the study area has been prepared from the intensive field surveys. The main lithological units of the study area are aphanetic and vesicular basalts, ignimbrite, tuffs, and quaternary sediments (alluvial, colluvial and residual soils). The ignimbrites and tuffs are highly altered and weathered and when they get water, they lose their shear strength and serve as lubricant for other overlaying lithology. Therefore, the degree and depth of weathering of each lithology have significant role for landslide initiations in the target area.

2.3.2.1.1 Geological structures

These structures were interpreted and compiled from satellite images, geophysical and geological field work surveys. Since the study area is found at the Afar Rift Margin which is worldwide known for its extensional tectonic movement and normal faults, then, faults are very important factor for the landslide problem of the study area. The western side of the study area is affected by active landslide problem because of the N-S directional fault. This part of the study area has a steep slope mountain by the action of fault and drainage system below it.

2.3.2.2 Topographical causes

2.3.2.2.1 Slope steepness

This is an important factor to cause landslide problem. In most landslides of the study area, steeper slopes have a greater chance of sliding problem but landslides are also common in the gentler slopes. The slope map of the area is derived from the 30m DEM using the slope function of the spatial analyst of ArcGIS 9.3. A map of slope classes is generated by grouping the slope angles into three major classes (Figure 2.19). The landslide in the area has occurred in all classes of slopes but dominant at the higher slope of the area.

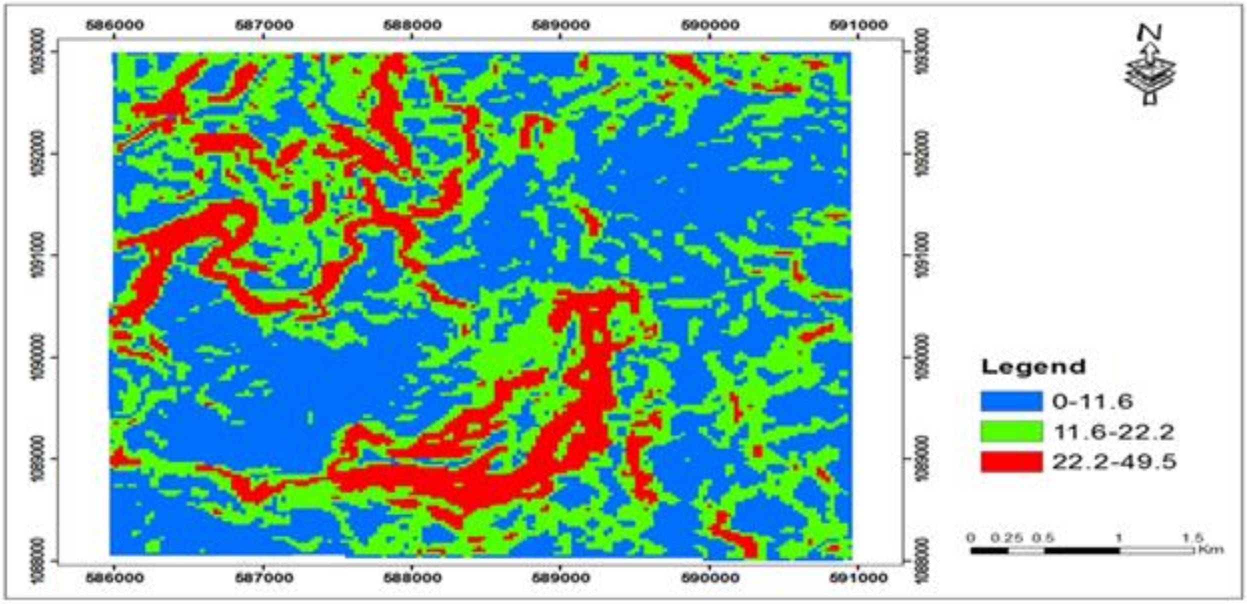

Figure 2.19 Slope angle map of the study area.

2.3.2.3 Hydro-meteorological causes

This plays a crucial role in landslide initiation. Some of the major significant hydrologic processes are discussed as follows:

2.3.2.3.1 Drainage systems of the study area

The drainage systems in study area outflow in all directions. Most drainage systems of the area have been created following the geological structures. The tectonic morphology of the study area is greatly modified by stream cuts, which finally could influence slope stability by over steepening the lower sections of the slopes and removal of materials that provided support at the toe. For this reason the drainage was considered as one causative factor in the landslide problem study.

2.3.2.3.2 Springs

Generally, the mountains of the study area are the sources of different springs. The main road of the interest area has also many seasonally and perennial springs which are emanates under the road. From the field observations, the main asphalt road is already failed to direction of the place where the springs are located. The study area has a higher potential of springs and groundwater and these are used as a lubricant and also can produce water pressures that cause landslides.

2.3.2.3.3 Rain fall

The slopes in the study area were mostly influenced by intermittent springs, rivers and high precipitation during rainy season. The most common trigger of landslide is sufficient water input during precipitation events. The mobilization of debris material during debris flow events is related either to the onset of sediment transport due to water runoff or to slope failures caused by an increase in pore-water pressures. Both runoff formation and slope instabilities are a function of rainfall intensity and cumulative precipitation or water input in another way. Rainfall and associated stream erosion are the main triggering factor of landslides.

2.3.2.4 Seismically causes

Earthquake is one of the principal triggering factors of landslides that cause great hazard to both of life and properties loss. The geological structures like dykes and faults of the study area are important situation for earthquake happening. Interviews with local people also confirmed that earthquake shake was felt around the study area. Thus, the most probable triggering factor for the landslide is the earthquake. Earthquakes reduce stability by imparting both a shearing stress and a reduction in resistance to slope material. The earthquake shocks may be responsible for triggering new landslides and reactivating old landslides.

2.3.2.5 Impact of landslide on the study area

The landslide problems caused by several factors have also several impacts on the property and main road of the locality of the study area. The principal impact was cracking and subsidence of the main road starting from Shola Meda up to Armania town which is around 3km coverage of the main road of the study area. Particularly at Shola Wuha locality (588353E, 1089748N), the landslide is active and the landslide scarps remains 90cm to reach the main asphalt road as shown in the first photographs of Annex-V. The remaining main road of the study area was also cracked and subsided in many parts of the localities (Annex-V).

The other impact of landslide in surrounding of the main road in the study area was also cracking of the foundation of national electric poles and many local houses of the study area (Annex-V). Most of the local houses have cracking of wall and floor and many of the residents change their houses to other palace. The national electric poles of the study area have also highly damaged particularly the poles at Shola Wuha and Tikure Chika localities which have cracked and subsiding foundations and have the tendency to fall down.

CHAPTER – THREE

THEORETICAL BACKGROUND OF GEOPHYSICAL METHODS

3.1 2D-Electrical Imaging Survey

3.1.1 Introduction

Recently, a new concept of instrumentation and data acquisition has been introduced to make it possible the acquisition of many readings in a reduced amount of time specifically for environmental applications corresponding to shallow investigations depths, of the order of 10 to 80m. The technique is sometimes called Electrical Resistivity Tomography (ERT). The concept involves using multi-core cables which contain as many individual wires as number of electrodes, with one take-out every 5m, 10m … and 24, 48, 72, 96 … electrodes. The measuring unit includes relays which automatically carry out the sequences of readings introduced in its internal memory. The aim of this set-up is to take readings for many combinations of transmission and reception pairs, so as to achieve some kind of mixed wenner / schlumberger array. In such a way of proceeding, the total length of cable is the product of the electrode spacing by the number of electrodes.

The greatest limitation of the resistivity sounding method is that it does not take into account horizontal changes in the subsurface resistivity. A more accurate model of the subsurface is a two-dimensional (2-D) model where the resistivity changes in the vertical direction, as well as in the horizontal direction along the survey line. In this case, it is assumed that resistivity does not change in the direction that is perpendicular to the survey line. In theory, a 3-D resistivity survey and interpretation model should be even more accurate. However, at the present time, 2-D surveys are the most practical economic compromise between obtaining very accurate results and keeping the survey costs down (Loke, 1999).

3.1.2 Instrumentation and Field survey

One of the new developments in recent years is the use of 2-D electrical imaging/tomography surveys to map areas with moderately complex geology (Griffiths and Barker, 1993). Such surveys are usually carried out using a large number of electrodes, 25 or more, connected to a multi-core cable. At present, field techniques and equipment to carry out 2-D resistivity surveys are well developed.

Figure 3.1 shows the typical setup for a 2-D survey with a number of electrodes along a straight line attached to a multi-core cable. Normally, a constant spacing between adjacent electrodes is used. The multi-core cable is attached to an electronic switching unit which is connected to a laptop computer. The sequence of measurements to take, the type of array to use and other survey parameters (such the current to use) is normally entered into a text file which can be read by a computer program in a laptop computer. After reading the control file, the computer program then automatically selects the appropriate electrodes for each measurement. One technique used to extend horizontally length covered of the survey, particularly for a system with a limited number of electrodes, is the roll along method (Figure 3.1). After completing the main sequence of measurements, one of cable is moved to the end of the line.

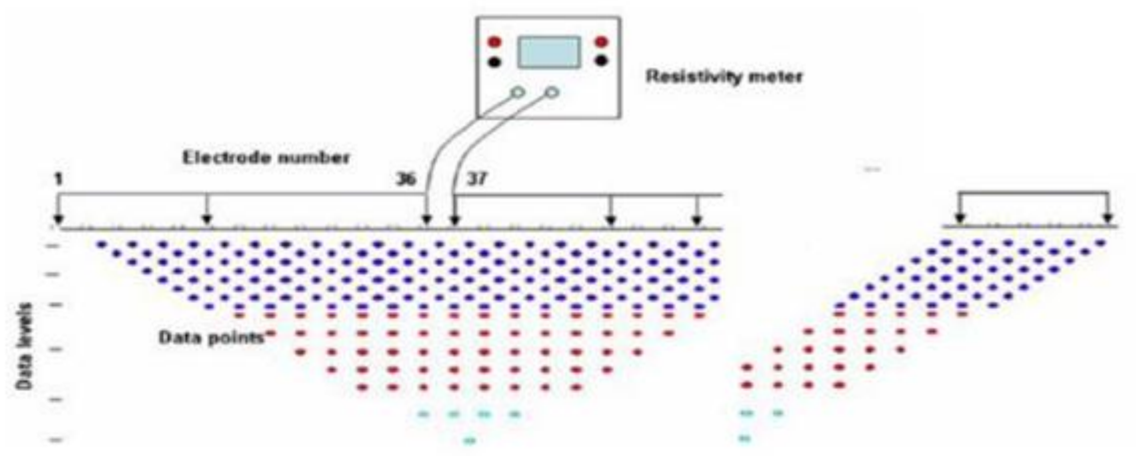

Figure 3.1 Generalized survey procedures with the main sequence in the left, roll along in the right and data points of 2-D resistivity imaging (Tigistu Haile, 2010).

3.1.3. Modeling of 2-D electrical resistivity imaging

Resistivity data is generally interpreted using the modeling process. A hypothetical model of the Earth and its geoelectrical section is generated. The theoretical electrical resistivity response over that model is then calculated. The theoretical response is then compared with the observed field response and the difference between the observed and calculated are noted. The hypothetical earth model is then adjusted to create a response which plausibly fit to the observed data.

3.1.3.1 Forward Modeling

Forward modeling is a technique to model a subsurface by estimating the actual resistivity of the different geological structures. The estimation is made by calculating the apparent resistivity of the respective ground structure using the fundamental theoretical electrical equations.

The resistivity response for a 2-D model is calculated and displayed as a pseudo-section for comparison with the original field data. This approach is used to generate realistic subsurface geometries in definable model structures (Reynolds, 1997). Forward modeling operates through a process which divides the subsurface into a large number of small rectangular cells (McDowell et al., 2002).

3.1.3.2 Basic Inverse Theory

Geophysical inversion is a method which finds a model that gives a response that is similar to the actual measured values. The model is an idealized mathematical representation of a section of the earth. The model has a set of model parameters of physical quantities which are required to be estimated from the observed data. The model response is the synthetic data that can be calculated from the mathematical relationships defining the model for a given set of model parameters. All inversion methods essentially try to determine a model for the subsurface whose response agrees with the measured data subject to certain restrictions.

In all optimization methods, an initial model is modified in an iterative manner so that the difference between the model response and the observed data values is reduced. The set of observed data can be written as a column vector **y** given by

$$y = col(y_1, y_2, \ldots y_m) \tag{3.1}$$

where **m** is the number of measurements. The model response **f** can be written in a similar form

$$f = col(f_1, f_2, \ldots f_m) \tag{3.2}$$

The difference between the observed data and the model response is given by discrepancy vector **g** that is defined by

$$g = y - f \tag{3.3}$$

In the least square optimization method, the initial model is modified such that the sum of squares error **e** of the difference between the model response and the observed data values is minimized and is given as (Loke, 1999).

$$e = \sum_{i=1}^{n} g^2 = g^T g \tag{3.4}$$

The above equation can be rewritten as

$$e = \sum_{i=1}^{n} \sqrt{(m_i - r_i)^2} \tag{3.5}$$

where, r_i is the i^{th} calculated reisitivity value, m_i is the i^{th} observed apparent resistivity and n is number of measured data. To get minimum **e** (root mean square error, RMS) the smoothness constrained least square method (deGroot-Hedlin and Constable, 1990) is used. It is given as

$$d\left(J^T J + U.F\right) = J^T g - UFr \tag{3.6}$$

where, $F = f_x f_x^T + f_z f_z^T$, f_x is vertical flatness filter, J is matrix of partial derivatives, U is damping factor, d is model perturbation factor, r is a vector containing the logarithm of the model resistivity value and g is discrepancy vector.

3.1.4 The relationship between geology and resistivity

Resistivity surveys give a picture of the subsurface resistivity distribution. To convert the resistivity picture to a geological picture, some knowledge of typical resistivity values for different types of subsurface materials and the geology of the area surveyed is important. Igneous and metamorphic rocks have high resistivity values, which greatly depend on degree of fracturing and the percentage of the fractures filled with water. Sedimentary rocks have lower resistivity value because they are usually porous and have higher water content (Annex-III).

3.2 The Magnetic Method

3.2.1 Introduction

Magnetic prospecting, the oldest method of geophysical exploration, is used for mineral, groundwater, oil and gas, engineering (locating buried structures and weak zones) and environment applications. It is a very popular and inexpensive approach for near-surface metal detection. Engineering and environmental site characterization often begin with a magnetometer survey as a means of rapidly providing a layer of information on where utilities and other buried concerns are located. The principal operation of magnetic survey is quite simple. When a ferrous material is placed within the Earth's magnetic field, it develops an induced magnetic field. The induced field is superimposed on the Earth's field at that location creating a magnetic anomaly.

Detection depends on the amount of magnetic material present and its distance from the sensor (Rivas, 2009).

3.2.2 Basic Principles and Elementary Theory

The Earth's large scale magnetic field is superimposed by small scale magnetic anomalies related with magnetized rocks. Magnetization is the parameter corresponding to density in the gravity method. Magnetization is a vector quantity which is related with the concept of north and South Pole of a magnet (Kirsch, 2009).

Within the vicinity of a bar magnet a magnetic flux is developed which flows from one end of the magnet to the other (Figure 3.2). This flux can be mapped rom the directions assumed by a small compass needle suspended within it. The points within the magnet where the flux converges are known as the poles of the magnet. A freely suspended bar magnet similarly aligns in the flux of the Earth's magnetic field. The pole of the magnet which tends to point in the direction of the Earth's North Pole is called positive pole, and this is balanced by the south seeking or negative pole (Kearey et al., 2002).

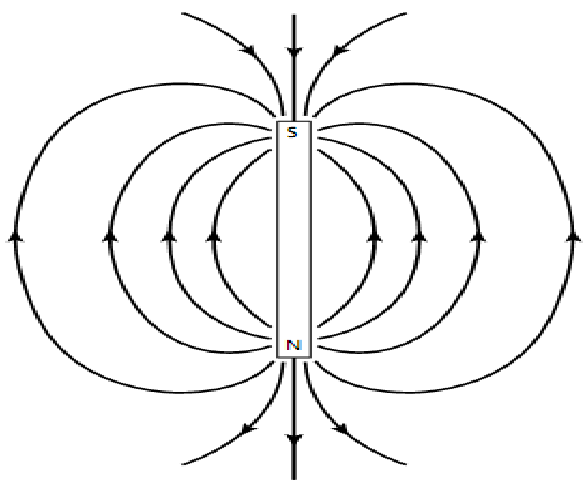

Figure 3.2 Magnetic flux surrounding a bar magnet (Kearey et al., 2002)

The force of **F** between two magnetic poles of strengths m_1 and m_2 separated by a distance r is given by

$$F = \frac{\mu_o m_1 m_2}{4\pi\mu_R r^2} \tag{3.7}$$

where μ_0 and μ_R are constants corresponding to the magnetic permeability of vacuum and the relative magnetic permeability of the medium separating the poles. The force is attractive if the poles are of different sign and repulsive if they are of like sign.

The magnetic field **B** due to a pole of strength m at a distance r from the pole is defined as the force exerted on unit positive pole at that point

$$B = \frac{\mu_o m}{4\pi\mu_R r^2} \tag{3.8}$$

Magnetic fields can be defined in terms of magnetic potentials. For a single pole of strength m, the potential **V** at a distance r from the pole is given by

$$V = \frac{\mu_o m}{4\pi\mu_R r} \tag{3.9}$$

The magnetic field component in any direction is then given by the partial derivative of the potential in that direction.

In the SI system of units, magnetic parameters are defined in terms of the flow of electric current. If a current is passed through a coil consisting of several turns of wire, magnetic flux flows through and around the coil annulus which arises from a magnetizing force **H.** The magnitude of **H is** proportional to the number of turns in the coil and the strength of the current, and inversely proportional to the length of the wire, so that **H** is expressed in Am^{-1}. The density of the magnetic flux, measured over an area perpendicular to the direction of flow, is known as the magnetic induction of magnetic field **B** of the coil. **B** is proportional to **H** and the constant of proportionality μ is known as the magnetic permeability (Reilly, 1972).

Common magnets exhibit a pair of poles and are therefore referred to as dipoles. The magnetic moment **M** of a dipole with poles of strength m a distance l apart is given by

$$M = ml \tag{3.10}$$

The magnetic moment of a current carrying coil is proportional to the number of turns in the coil, its cross-sectional area and the magnitude of the current.

When a material is placed in a magnetic field it may acquire a magnetization. This phenomenon is referred to as induced magnetization. The intensity of induced magnetization **J** of a material is defined as the dipole moment per unit volume of the material

$$J = \frac{M}{LA} \tag{3.11}$$

In other way the induced intensity of magnetization is proportional to the strength of the magnetizing force **H** of the inducing field.

$$J = \kappa H \tag{3.12}$$

where, **K** is the magnetic susceptibility of the material.

In a vacuum the magnetic field strength **B** and magnetizing force **H** are related by

$$B = \mu_o H \tag{3.13}$$

where, μ_0 is the permeability of vacuum ($4\pi \times 10^{-7} Hm^{-1}$). Air and water have similar permeability to μ_0 and so this relationship can be taken to represent the Earth's magnetic field when it is undisturbed by magnetic materials. When a magnetic material is placed in this field, the resulting magnetization gives rise to an additional magnetic field in the region occupied by the material, whose strength is given by $\mu_0 J$. Within the body the total magnetic field or magnetic induction, **B** is given by

$$B = \mu_o H + \mu_o J \tag{3.14}$$

Substituting equation (3.14)

$$B = \mu_o H + \mu_o \kappa H = (1+\kappa)\mu_o H = \mu_R \mu_o H$$

The magnetic permeability **μ**is thus equal to the product of the relative permeability and the permeability of vacuum, and has the same dimensions as $\boldsymbol{\mu_0}$**.** For air and water μ_R is close to unity.

3.2.3 The Earth's Magnetic field

The geomagnetic field near the surface of the Earth originates largely from within and around the Earth's core. Ninety percent of the Earth's magnetic field looks like a magnetic field that would be generated from a dipolar magnetic source located at the center of the Earth and aligned with the

Earth's rotational axis. The remaining 10% of the magnetic field cannot be explained in terms of simple dipolar sources. Complex models of the Earth's magnetic field have been developed and are available. As observed on the surface of the Earth, the magnetic field can be broken into three separate components.

Main Field: This is the largest component of the magnetic field and is believed to be caused by electrical currents in the Earth's fluid outer core. It is produced in the core of the earth and accounts for the very large regional variations in the field intensity and direction. For exploration work, this field acts as the inducing magnetic field.

External Magnetic Field: This is a relatively small portion of the observed magnetic field that is generated from magnetic sources external to the earth. This field is believed to be produced by interactions of the Earth's ionosphere with the solar wind. Hence, temporal variations associated with the external magnetic field are correlated to solar activity.

Crustal Field (Anomalous Magnetic Field): This is the portion of the magnetic field associated with the magnetism of crustal rocks. This portion of the field contains both magnetism caused by the induction of Earth's main magnetic field and remnant magnetization (Thomas, 2003). Mathematically it can be expressed by:

$$B_T = B_{ext} + B_{\mathrm{int}} = B_{ext} + B_D + B_{rm} \qquad (3.15)$$

where B_T is the total magnetic field, B_{ext} is external magnetic field, B_D is dipole field, which is mainly generated by the fluid outer core and Brm is the field of rock magnetism.

3.2.4 Temporal Variation of Earth’s magnetic field

It was recognized that the earth's magnetic intensity changes its direction slowly and irregularly. Later measurements at magnetic observatories showed many changes in the magnetic field that have shorter periods than those originally observed. This temporal variation may be resolved into secular variation, diurnal variation and variations due to magnetic storms.

Secular variation: These are long-term (changes in the field that occur over years) variations in the main magnetic field that are presumably caused by fluid motion in the Earth's outer core. These variations occur slowly with respect to the time of completion of a typical exploration magnetic survey; as result .these variations will not complicate data reduction efforts.

Diurnal variation: These variations in the magnetic field that occur over the course of a day and related to variations in the Earth's external magnetic field. This variation can be 20 to 30nT per day and accounted for when conducting exploration magnetic surveys. Diurnal variations are believed to be caused by electric currents induced in the Earth from an external source.

Magnetic storms: Magnetic activity, occasionally in the ionosphere will abruptly increase, the occurrence of such storms correlates with enhanced sunspot activity. The magnetic field observed during these times is highly irregular and unpredictable, having amplitudes 1000nT. Magnetic surveying should be discontinued during such storms because of the impossibility of correcting the data collected for the rapid and high–amplitude changes in the magnetic field (Kearey, Brooks and Hill, 2002).

3.2.5 Magnetics Surveys Instrument

Magnetic field measurements are carried out with magnetometers. Magnetometers measure horizontal and/or vertical components of the magnetic field or the total field. There are two main types of resonance magnetometer: the proton free-precession magnetometer, which is the best known, and the alkali vapour magnetometer. Both types monitor the precession of atomic particles in an ambient magnetic field to provide an absolute measure of the total magnetic field (F). The proton magnetometer has a sensor which consists of a bottle containing a proton-rich liquid, usually water or kerosene, around which a coil is wrapped, connected to the measuring apparatus (Reynolds, 1997). Proton precession magnetometers measure the total intensity of the Earth's magnetic field vector at a resolution of 0.1–1nT (Kirsch, 2009).

3.2.6 Magnetic field survey procedure

The aim of magnetic survey is to investigate subsurface geology on the basis of anomalies in the Earth's magnetic field resulting from the magnetic properties of the underling rocks. A survey can be performed on land, at sea and in the air. Consequently, the technique is widely employed and the speed of operation makes the method very attractive (Kearey et al., 2002). Magnetic measurements are performed in grids or on profiles. Repeated magnetometer readings at base station have to be performed to record periodic and non periodic magnetic fluctuations related with ionospheric processes (Kirsch, 2009).

The method involves the measurement of variations in the total magnetic field of the earth, caused by local differences in the magnetization of the subsurface rocks and soils. The greatest application in engineering studies is it locates boundaries between rocks, which display magnetic contrasts, such as faults or dykes. Significant progress has been made in the mathematical modeling of magnetic data, particularly of the variations in 1-D visualization. It is also possible to produce 2-D geological models from the magnetic data (McDowell et al., 2002).

In ground based surveys, it is important to establish a local base station in an area away from suspected magnetic targets or magnetic noise and where the locale field gradient is relatively flat. A base station should be quick and easy to relocate and reoccupy. The precise approach to the survey will depend on the type of equipments. If a manual push button proton magnetometer is deployed, the exact time of occupation of each station is needed and at least three reading of the total field strength should be recorded. Each of the three values should be within ± 1or 2nT and then an average of these three readings is calculated. As the survey progresses, the base station must be reoccupied every half an hour in order to compile a diurnal variation curve for later correction. Next to data entry, where required, there should be any comments about the terrain or other factors that may be considered to be important or relevant to subsequent data processing and interpretation (Reynolds, 1997).

3.2.7 Magnetic Data Reduction

The Earth’s magnetic field changes over a daily period and these are what are called the diurnal variations. These are caused by changes in the strength and direction of currents in the ionosphere. On a magnetically quiet day, the changes are on average around 50nT but with maximum amplitudes up to 200nT at the geomagnetic equator (Reynolds, 1997). Therefore, one effect that must be compensated in magnetic survey is the variation in intensity of the geomagnetic field at the Earth’s surface during the course of a day which is diurnal variation. It can be corrected by installing a constantly recording magnetometer at a fixed base station within the survey area by visiting a base station periodically (Lowrie, 2007).

The geomagnetic correction is a technique that removes the effect of geomagnetic references field from the survey data. The most rigorous method of geomagnetic correction is the use of the International Geomagnetic Reference Field (IGRF) (Kearey et al., 2002). For small sized area of investigation only diurnal corrections could be applied (Kirsch, 2009). The total field anomaly ($\mathbf{\Delta B}$) is calculated based on the following formula from the observed magnetic data ($\mathbf{B_{obs}}$), the diurnal variation ($\mathbf{\delta B}$) which, will be generated from the base station measurement and the dipole field ($\mathbf{B_d}$) which will be determined from the international geomagnetic reference field.

$$\Delta B = B_{obs} \pm \delta B - B_d \tag{3.16}$$

3.2.8 Analytical Signal

Due to the dipolar nature of the geomagnetic field, magnetic anomalies observed anywhere other than the poles are asymmetric even when the causative body distribution is symmetric. This property complicates the interpretation of magnetic data. Analytical signal is a suitable quantity that can be calculated in frequency domain and its magnitude is independent of the magnetization direction. Analytical signal is formed through the combination of the horizontal and vertical gradient of the magnetic anomaly. The analytical signal has a form over causative body that depends on the location of the body (horizontal coordinates and depth) but not on its magnetization direction (Roest et al., 1992).

The acquired anomaly is therefore the one that would be measured at the north magnetic pole, where induced magnetization and ambient field both are directed downwards (Blakely, 1995). The amplitude function of the analytical signal is defined as the square root of the squared sum of the vertical and two horizontal derivatives of the magnetic field anomaly:

$$|\, A(x, y) \,| = \sqrt{\left(\frac{\partial M}{\partial x}\right)^2 + \left(\frac{\partial M}{\partial y}\right)^2 + \left(\frac{\partial M}{\partial z}\right)^2}$$

where |A(x, y)| and M are the amplitudes of the analytic signal and the magnetic anomaly field intensity respectively. This signal exhibits maxima over magnetization contrasts, independent of the ambient magnetic field and source magnetization directions (Salem et al., 2002).

3.2.9 Magnetic properties of rocks and minerals

Magnetism of rocks is related with the magnetism of the rock forming minerals. Diamagnetic minerals like quartz and calcite have negative susceptibilities of the order of 10^{-5}. Minerals like feldspars and micas are paramagnetic and have higher (positive) susceptibilities ($10^{-4} – 10^{-2}$). The positive susceptibility of ferromagnetic minerals like magnetite (k ~ 1 - 10) is even larger by some orders of magnitude and in general most important for the magnetization of rocks (Kirsch, 2009).

Magnetic susceptibility is an extremely important property of rocks and to magnetic exploration method. The whole rock susceptibility can vary considerably owing to a number of factors in addition to mineralogical composition such as alignment and shape of the magnetic grains dispersed throughout the rock (Reynolds, 1997).

However the susceptibility of a rock mainly depends on its magnetite content. Sediments and acidic igneous rocks have small susceptibilities whereas basalts, dolerites, gabbros and serpentinites are usually strongly magnetic. Weathering generally reduces susceptibility because magnetite is oxidized to hematite. The susceptibilities, in rationalized SI units, of some common rocks and minerals are given in Annex- III (Milson, 2003).

CHAPTER - FOUR

GEOPHYSICAL INVESTIGATIONS OF THE STUDY AREA

4.1 Electrical Resistivity Tomography (ERT)

4.1.1 ERT Data Acquisition and Instrumentation

Three profiles were surveyed to collect ERT data parallel to the main road of study area. Profile-1 covers 360m horizontal distance and the other two profiles also cover 450m each. The ERT survey was conducted to study the subsurface condition of the road in order to delineate the sliding surface and also provide information about the associated processes on the basis of the contrasts in the subsurface resistivities.

The electrical resistivity data was collected using the IRIS instruments SYSCAL R1 plus Switch 72 resistivity meter that utilizes 72 electrodes, through interconnectable four reel cables accommodating 18 electrodes each, 72 short connector wires and two reversible connector boxes (Figure 4.1). The cables used in the particular instrumentation have pick up/connection points spaced at 5m. The instrument records automatically with a present format uploaded into the unit and the system takes measurements almost independently once the arrays are laid along the profile.

Figure 4.1 Instrumentation of 2D electrical imaging.

Reel cables are connected each other with connector boxes and each cable outlet is connected to electrode by the connector wires. A twelve volt external battery was used for this survey. In the survey, the instrument is normally put at the center, where the deepest depth is recorded, and the four cables reels spread on both side of the resistivity meter. The two cables are in one side of the resistivity meter while the other two are spread on the other side of the resistivity meter (Figure 4.2).

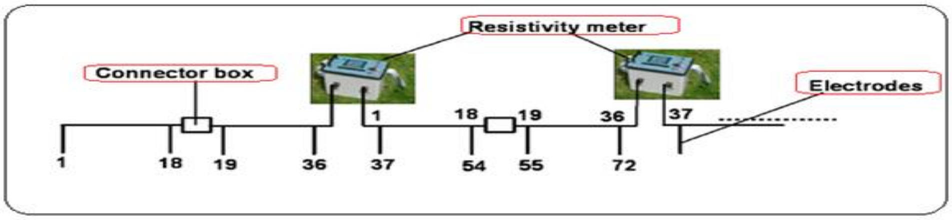

Figure 4.2 General Field layout of 2D electrical imaging, the bottom electrodes for the main sequence where as the top electrodes for the roll along.

The three parallel profiles are about 50m apart. The first profile (P_1) is 100m distant above the road and it is surveyed by one main sequence which covers a horizontal distance of 360m. The other two profiles P_2 and P_3, which are parallel to P_1, are positioned above the road and down the road respectively. These two profiles P_2 and P_3 are surveyed by one main and one roll along sequences which covers a horizontal distance of 450m and contains 945 data points each. The main sequence contains 648 data points covering 360m horizontal distance while each of the roll along sequences contain 297 data points covering a horizontal distance of 90m.

Table 4.1 Acquisition parameters for the ERT survey.

Parameter	ERT Profile 1	ERT Profile 2	ERT Profile 3
Electrode spacing (m)	5	5	5
Length of profile (m)	360	450	450
Number of electrodes	72	90	90
Number of data points	648	945	945
Array type		Schlumberger Wenner	
Equipments		SYSCAL R1 Plus Switch 72	
Sequence type	Main	Main and Roll Along	Main and Roll Along

4.1.2 Data Processing and Presentation

The data generated at field from each main and roll along sequences are downloaded to a computer using the Prosys-II software. Then the data from each roll along sequence is added to the main sequence before the processing stage with the help of this software. After the summation, the summed data is filtered, by automatic filtering, and the noisy data is rejected. Finally the filtered data is saved in the Prosys-II software in ".dat" form and exported to RES2DINV software for processing. An automatic iteration process that fits the modeled data with the calculated one proceeds to analyze the data. The final output of RES2DINV software, the inverted 2D model resistivity section, is the processing product of 2D survey (Figure 5.1b). Finally such figures are used for interpretation purpose and to correlate the results of 2D imaging analysis with results of other methods.

The data obtained in the prosys–II software is started from 90m for each roll along. Because of this, the roll along sequences were adjusted with proper distance before add to the main sequence. In the case of roll along one the data started from 90m, so no distance adjustment is needed. The second roll along sequence data sheet was recorded after 90 meter of the first roll along data; it was shifted by 90 meter after getting in the Prosys-II software. This step was continued for the rest roll along data by increasing total roll along distance by 90 meter that means 180m to the 3rd roll along, 270m to the 4th roll along and 360m to the 5th roll along. After adjusting the distance, the rolls along sequences were added to the main sequence. Topography was incorporated to the 2D electrical resistivity section because the project site is on undulating terrain.

4.2 Magnetic method

4.2.1 Data acquisition and Instrumentation

Magnetic data were collected using Proton Precision Magnetometer instrument. The surveying was stated by establishment of a base station within the study area at a place which is easily accessible and as far as possible from magnetic noise. In addition to the magnetic readings the geographic coordinates of the point at which the readings are taken and the time of reading was recorded using Global Positioning System (GPS). Similar to that of the electrical resistivity data, magnetic data were also collected along the predefined profile lines, which were used to conduct electrical resistivity surveys. In addition, magnetic data are also collected randomly within and at the boundary of the study area. Magnetic data were collected from 158 data points with average spacing of 15m along the selected profile lines and at random points. At the field survey three magnetic readings were taken for a specific point and then average of this readings were used for the processing and interpretation purpose (Figure 4.3).

4.2.2 Magnetic data processing and presentation

The diurnal variation was removed from the observed magnetic field data using the Microsoft excel 2010. The main magnetic field at the base station is obtained from the International Geomagnetic Reference Field (IGRF). The IGRF value of the area was 35907.61. The IGRF value at the base station is subtracted from the diurnal corrected total magnetic field of each station. Finally, the corrected magnetic anomaly was obtained by subtracting the diurnal variation and IGRF values from the survey data. This was used for processing to produce anomaly map, profile plots, analytical, and horizontal gradient maps and finally magnetic modeling maps.

Magnetic profile data were picked up from the magnetic anomaly map corresponding to the profiles of the 2D electrical resistivity imaging lines. This helps to counter check and integrating the results from the two methods for detail interpretations.

Since the study area is found within the low latitude magnetic equator and the survey covers very small area, then the variation of magnetic field with latitude and longitude is insignificant and hence normal corrections were done. In addition to this, in magnetic equatorial regions where inclination is less than 15 degrees, reduction to the pole is generally unstable and cannot be derived (Getech, 2007). Due to this reason reduction to the pole was not also done. Rather than reduction to the pole and normal corrections, other data enhancement technique was applied to produce magnetic map, which may help to highlight particular characteristics or features to aid qualitative interpretation. Analytic signal was done by using Geosoft software package program called MAGMAP.

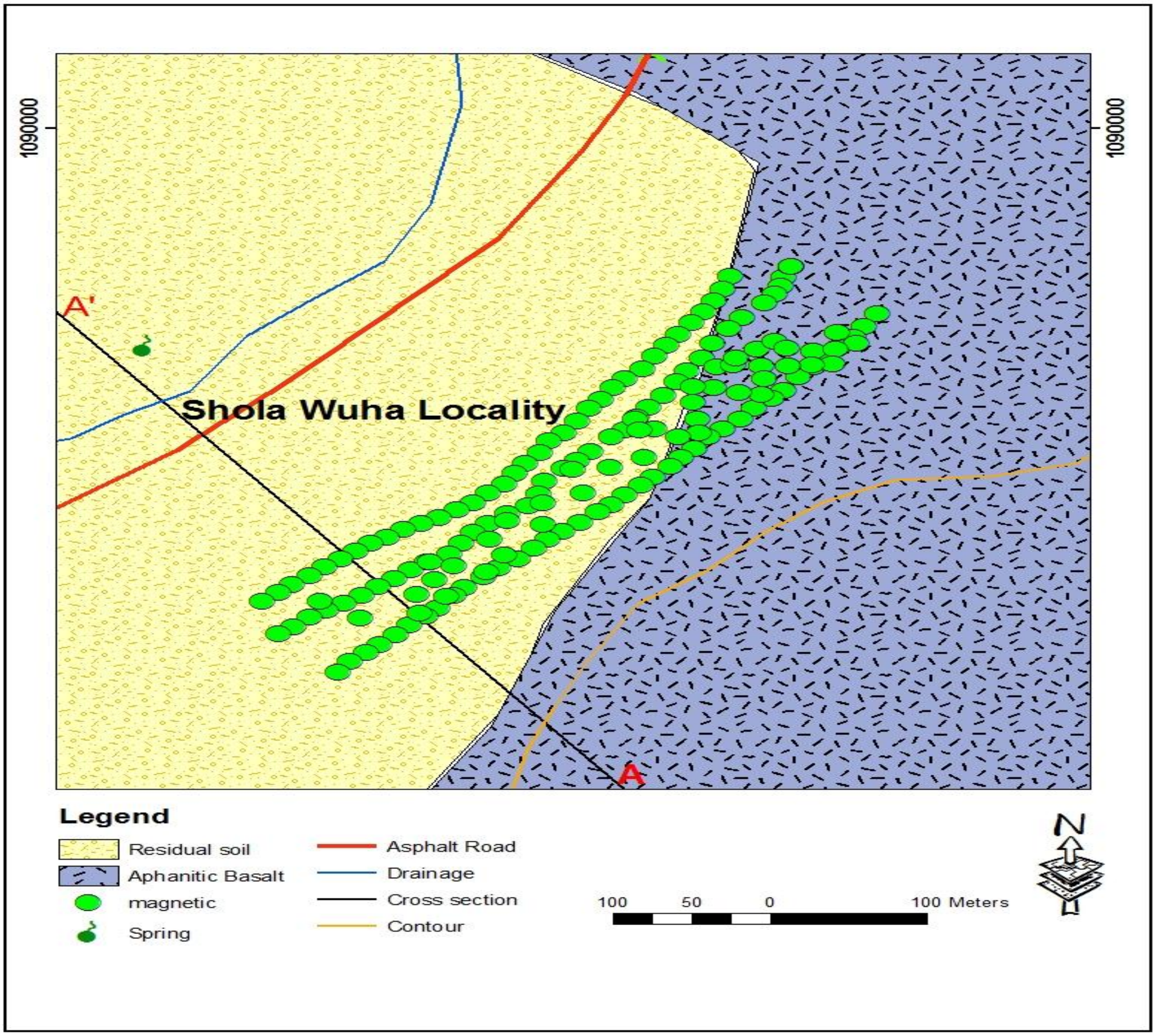

Figure 4.3 Magnetic data distribution map overlay on enlarged grid of geological map of the area.

CHAPTER - FIVE

RESULTS AND JOINT INTERPRETATIONS

5.1 Electrical Resistivity Tomography and Magnetic Profiles

5.1.1 Introduction

Geophysical investigations were surveyed at the above and down of the affected road, and have important information about the sliding surface of study area and geological weak zones. These results illustrate the benefits of electrical resistivity imaging techniques for characterizing the landslide problem. Since the layers in the inverse model of imaging have highly disturbed and fragmented subsurfaces, then it was difficult to correlate with the vertical lithological stratification of the study area and with magnetic profiles models. Because of the depth difference and deep landslide disturbance problem, the correlations of geoelectrical sections with the vertical geological layers and magnetic models were not done but the individual magnetic profiles have good correlation with electrical imaging models in indicating geological structures of the surveyed area.

5.1.1.1 Profile-1

The inversion of profile one by including topography was done after filtering and removing of the noisy data from 648 data points of the 2D electrical resistivity of profile-1, 600 data points were used for the inversion of this profile. The profile was only main sequence and with total length of the profile extended to 360m, and its inversion result is given in the Figure 5.1. The program produced a good inverse model after six iterations and 3% RMS errors. The resistivity inverse model of profile-1 has a lot of disturbed zones which have high susceptibility to slide and different geological structures that are suitable conditions for landslide happening.

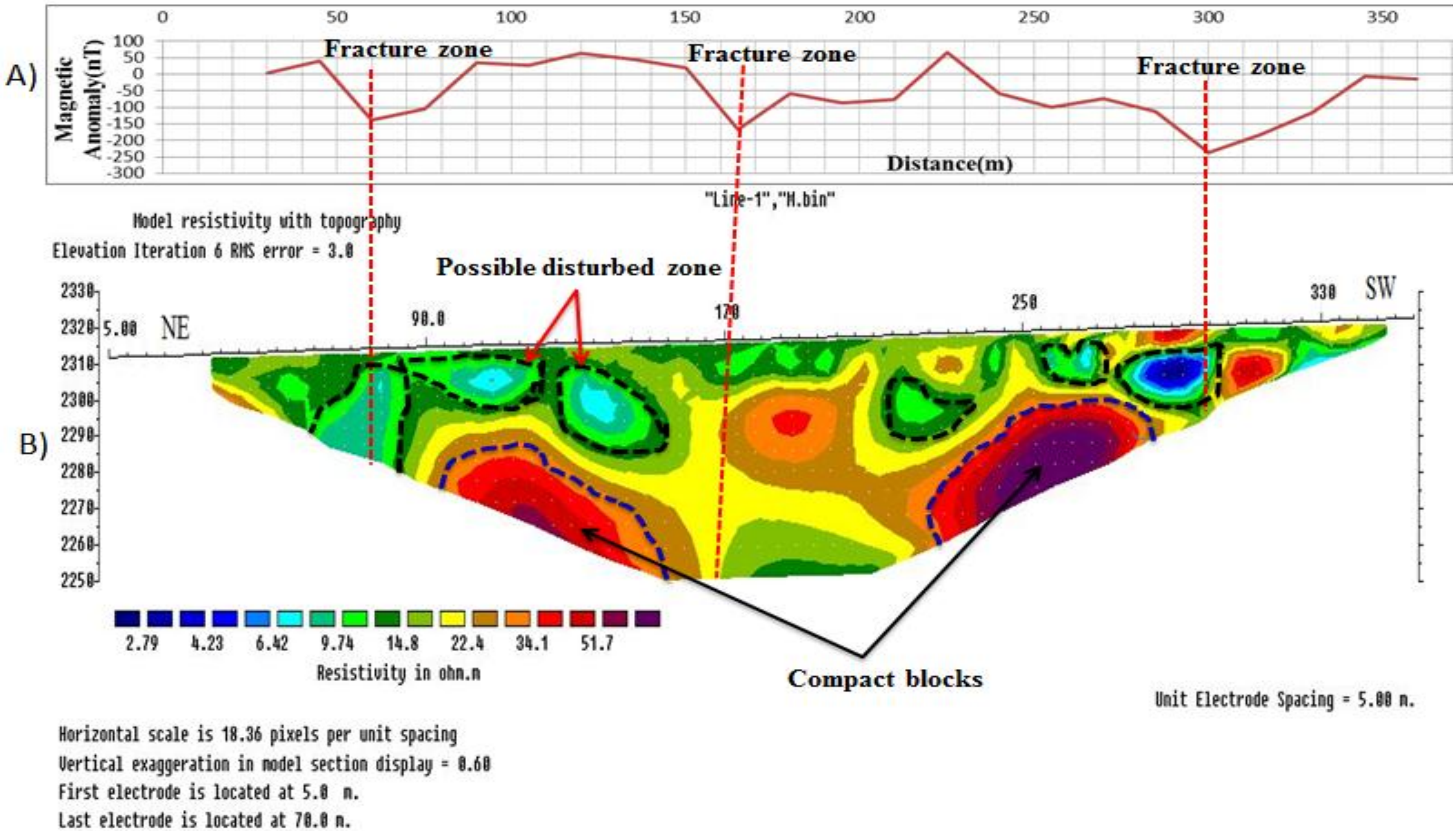

Figure 5.1 Interpretation of profile-1 a) magnetic profile, b) 2D electrical resistivity section.

The resistivity value of the possible disturbed subsurfaces and geological weak zones is very low and varies from 2.79 to 14.8 Ωm. This low resistivity in some of the areas within the profile line is possibly due to intensive degree of weathering and water percolation from the surface along the fractures. In addition to this, these resistivity ranges are the response of fragmenting and sliding surface, which is composed of expansive dark clay and highly to completely weathered basalt rock. The thickness of this disturbed and susceptible to slide surface increases from southwestern to northeastern directions.-.

The second ranges of resistivity is from 14.8 – 34.1 Ωm and this may be the response of the highly to completely weathered and fractured ignimbrite rock. This range of resistivity value has indicated subsurface geology that are easily weathered and disintegrated into fragments of blocks and the presence of weak zones. The thickness of this range of resistivity is deeper in the center of the profile and in locations where weak zones are found.

The third range of resistivity is greater than 34.1 Ωm which is the response of the compacted blocks. These massive blocks which maybe bed rocks have dislocated at the center of the profile by the intrusion of geological structures may be faults. Depth to the compact rock is varying due to the presence of deep geological structures. It is shallower in the southwestern side as compared with the northeastern side of the 2D electrical profile.

The magnetic profile along the 2D electrical imaging of profile-1 was plotted as shown in the Figure 5.1a. This profile shows considerable amplitude variation in the magnetic anomaly signatures. The minimum negative peak value is -236.15nT at a distance of about 300m and the maximum positive peak value is 65.34nT at a distance of about 225m from the northeastern end of the line. There is a positive correlation between the magnetic anomaly plot and the 2D electrical profile in detecting the weak zones. The magnetic anomaly plot shows a presence of fractured zone at 75m, 170m and 300m of the profile which are also interpreted same from the 2D electrical imaging plot.

5.1.1.2 Profile-2

The inverted model resistivity with topography was done after filtering out the noisy data from the 945 resistivity raw data points, a total of 908 data points were used for the inversion. Integrating the main and one roll along sequences and covers 450m length of the profile to produce the inversion section plot shown in Figure 5.2. The software has applied inverse model by iterating just seven times to yield a quality data with RMS error of 2.1 %. This profile could be classified into three ranges of resistivity value by carefully examine the entire depth resistivity informations.

The first range shows a very low resistivity anomaly that varies from 5.22 to 13.4 Ωm. This range of resistivity is almost similar to the first profile-1 which has a fragmented and sliding surface of expansive clay and highly weathered basalt rock. Like profile-1, the thickness of this resistivity range increases from southwest to northeast direction of profilr-2. The greater thickness of disturbed and sliding surface is located at northeast direction and this could be due to the high degree of weathering and weak zones along this direction.

The second range of resistivity is from 13.4 to 21.4 Ωm which may possibly the response of moderately to highly weathered ignimbrite rock. This range of resistivity is localized in between 165 and 245m horizontal distances and some extent towards SW direction. The thickness has increased at the center and decreased to SW direction. This range value has no extent towards NE direction and this may be due to sliding problem and accumulation of clay soils and slide deposits at this location. The thickness where this range of resistivity is located at this profile become greater in comparison to other profiles due to the presence of weak zones which are attributed to the intensively weathered and fractured earth materials resulting a fragments of rocks.

The third range of resistivity is greater than 21.4 Ωm which may possibly the response of massive basalt rock. This massive block of basalt rock is characterized by large depth at northeastern direction but shallower in the southwestern of the 2D electrical resistivity profile as shown in Figure 5.2. This compact rock is again broken equivalently to the massive rock mapped in profile-1. The two small blocks on the two end of the profile are dissected by weak zone and similarly, one block from the compact rock at the center of the profile is also displaced by localized structures. Therefore, the weak zone and slope factor may possibly interpret as deriving force for sliding problem at this profile and in other profile as well. The locations of these weak zones are intense at NE direction of this profile.

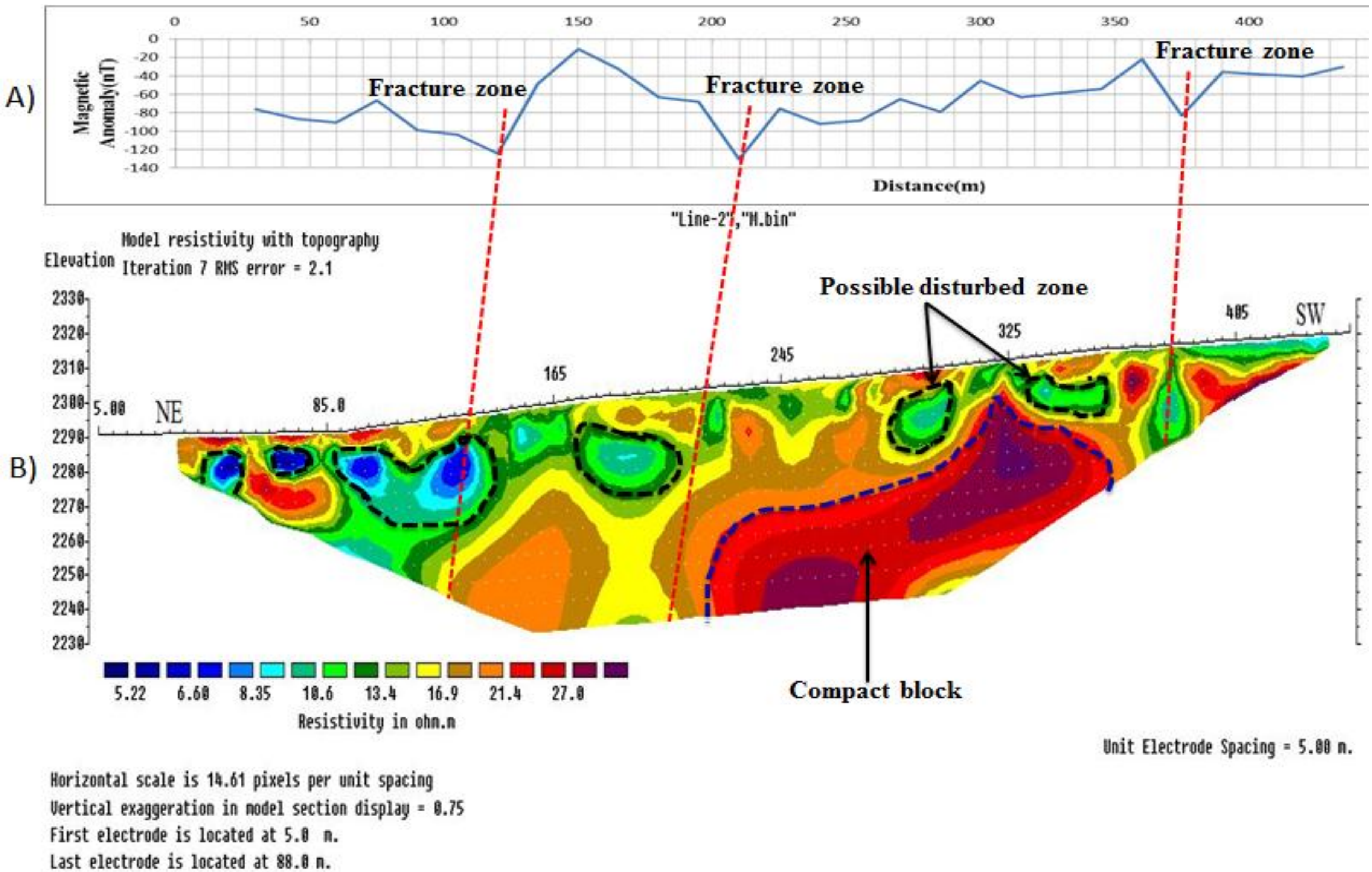

Figure 5.2 Interpretation of profile-2 a) magnetic profile, b) 2D electrical resistivity section.

The magnetic profile along the 2D electrical imaging profile-2 is also plotted as shown in the top section of the 2D image in Figure 5.2a. The extreme values whose minimum negative peak value of -130.21nT at a distance of about 210m and the maximum positive peak value of -11.15nT at a distance of about 150m from northeastern end point of the profile. The magnetic field profile almost coincides with the 2D electrical resistivity imaging model in identifying the fracture zones. The magnetic profile plot shows the presence of fracture zones in almost at three parts of the profile survey and these are confirmed by electrical imaging model profile.

5.1.1.3 Profile-3

An important feature of this image is the vertical decrease in resistivity with depth, where low resistivity range values are reached beyond the depth investigation of the instrument. This result suggests that the presence of massive rock at deeper depth than the other profiles. The inverted model resistivity with topography was done after filtering out the noisy data from the 945 resistivity raw data points, a total of 891 data points were used for the inversion model. The length of this profile is again 450m resulting from a combination of a main and one roll along sequences. The inversion result is shown in Figure 5.3. The software produced good inverse model after iteration of about seven times and showing a good data quality with RMS error of 2.8%. This profile could be again classified into three resistivity value ranges in agreement with the other two profiles but with great variations in depth of the resistivity range values.

The obtained inversion model with topography from this line is characterized by a high degree of disturbances and huge thickness of alluvial, colluvial and residual soil deposits. Along the profile, the low range resistivity value is varies from 4.32 to 20 Ωm and these resistivity responses are that of the dark expansive clay soil and due to intensive degree of weathering and water percolation from the surface along the fractures . As compared with the low resistivity range value in the other two profiles, this value of range is relatively thicker and localized at NE of the profile and also deposited under the fragmented boulders of basalt rock towards the southwest direction. This low resistivity soils are deposited at the whole profile especially at the lower depth and are almost absent at the shallow depth of NE direction of the profile starting from 245m and above horizontal distance. From center of the profile to the direction of SW, the disturbed and fragmented blocks are suspended and sliding following the sloped surface above this low range resistivity values.

The second resistivity range varies from 20 – 43Ωm which may be the response of the slightly to highly weathered and fractured ignimbrite rock. Generally, the thickness of this value in NE direction is disappeared and there is an indication of this resistivity value in the SW direction of this profile.

The third resistivity value is found only at shallower depth of SW direction of the profile with highly fractured, fragmented and weathered blocks that shows a significant resistivity variation within it. The suspended blocks that have this resistivity range value have the tendency to slide down the slope especially in NE direction of the profile.

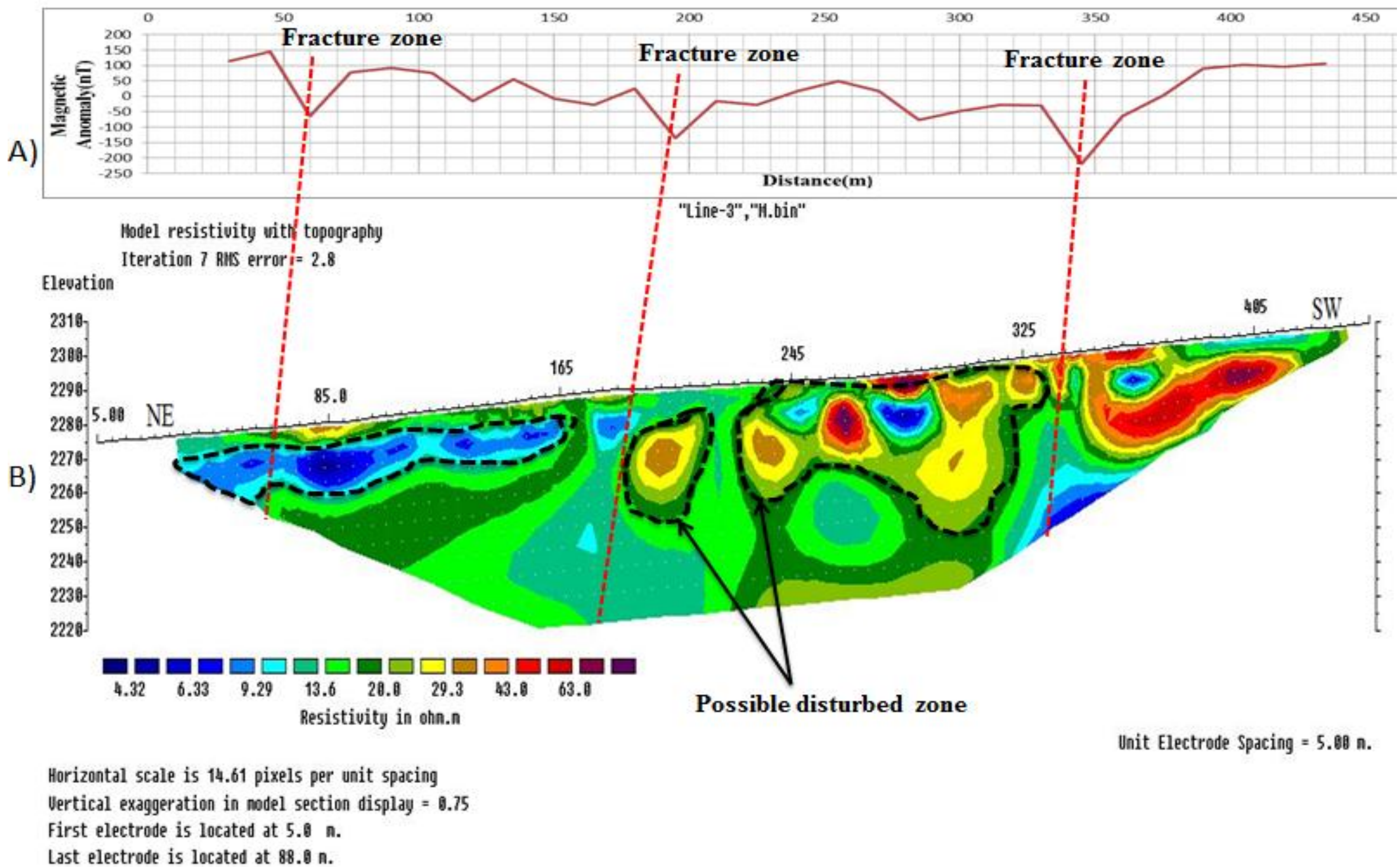

Figure 5.3 Interpretation of profile-3 a) magnetic profile, b) 2D electrical resistivity section.

There is also very low resistivity zone at the bottom of the third resistivity range value of SW direction of the profile. Generally, the low resistivity range is dominantly cover almost the whole profile horizontally and vertically extents which may possibly due to high degree of weathering and water percolation from the surface along the fractures.

Magnetic profile along the same line on which 2D electrical imaging of profile-3 was plotted as shown on the top of the inverted resistivity model (Figure 5.3a). The minimum negative peak value is -218.27nT at a distance of about 345m and the maximum positive peak value is 144.16nT at a distance of about 45m from the initial station position on the northeastern side of the line. The magnetic field profile roughly coincides with the 2D electrical resistivity profile plot to identify the fracture zones. The magnetic profile clearly shows the presence of two fractured zones which could also be interpreted same to other two 2D electrical resistivity sections.

5.1.1.4 Combination of the 2D electrical resistivity profiles

Figure 5.4 illustrates how the three 2D electrical resistivity sections of profile-1, profile-2 and profile-3 can be arranged horizontally to give a full of representation of the area. This way of representation is important to understand the continuity of the sliding surface and weak zones within the survey area. The plot clearly depicts that there is continuous fractured zone within the three profiles shown in Figure 5.4. There are also possibly rotational sliding shallow subsurfaces in all the three profiles. The there is an occurrence of landslide especially in northeast direction of profile three which clearly correlate with failure section of the road.

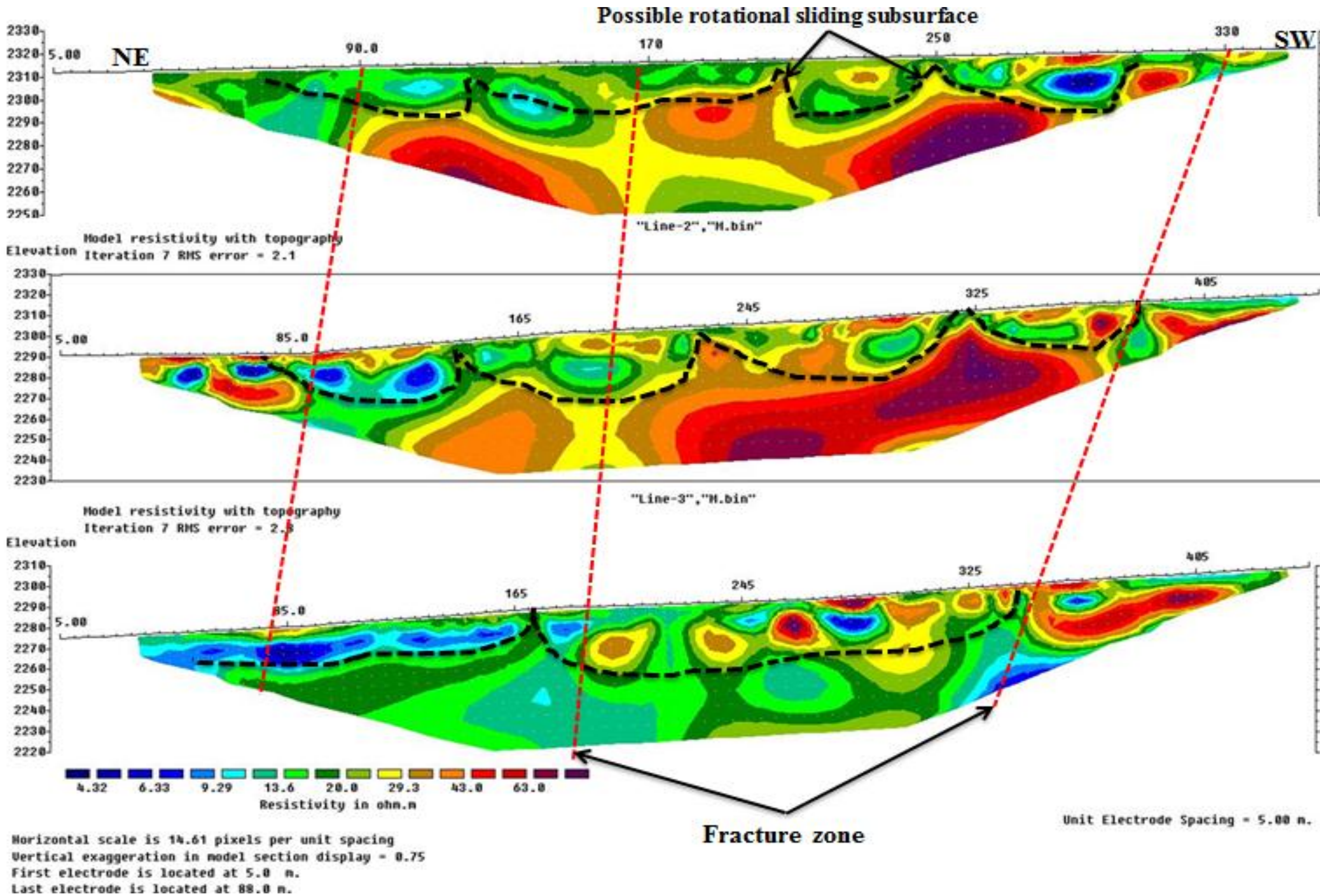

Figure 5.4 the net representation of Profile-1, Profile-2 and Profile-3 together with their sliding subsurface.

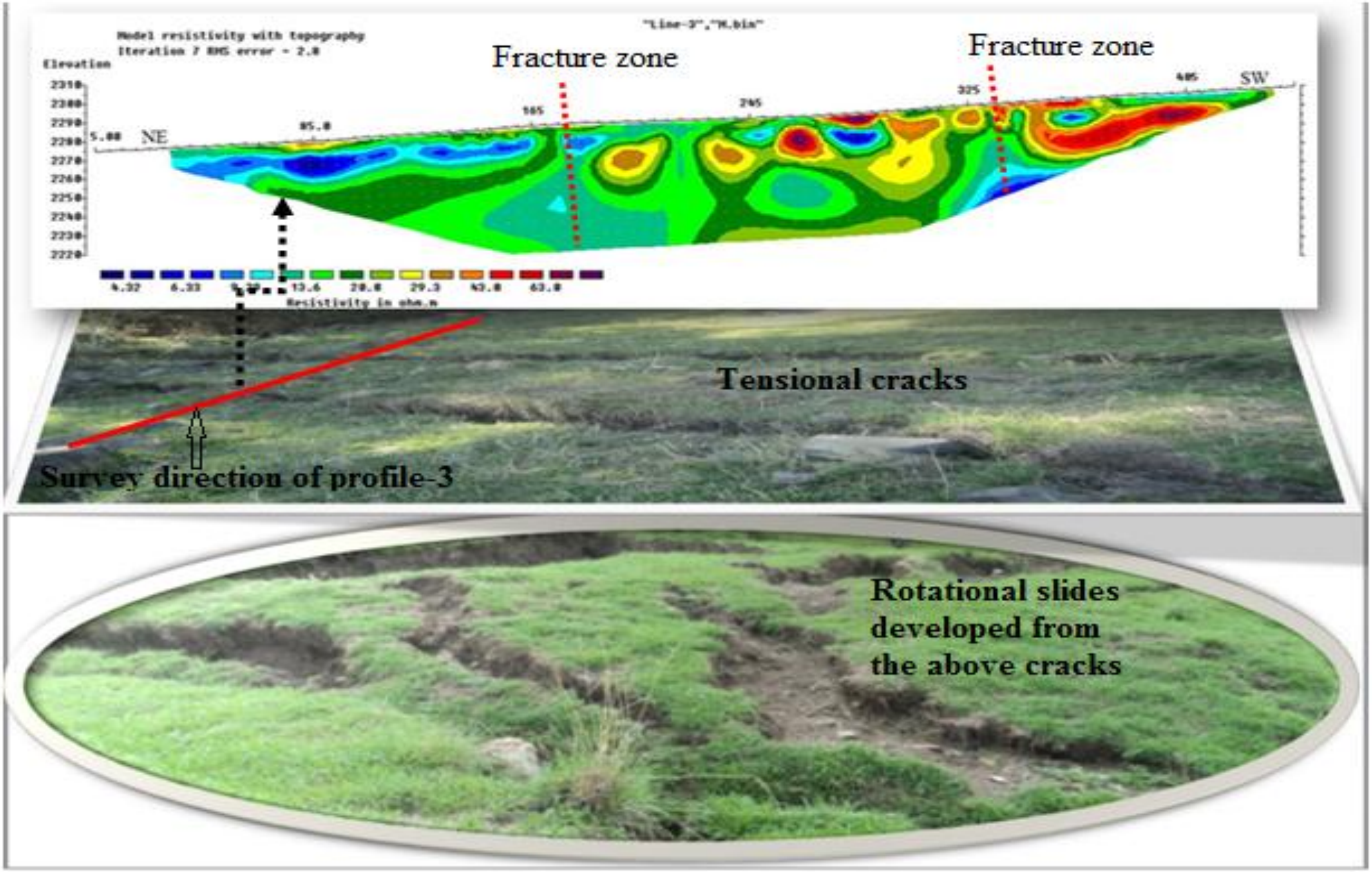

Figure 5.5 correlating of model resistivity of profile-3 with the surface sliding problem of the main road

5.2 Magnetic Data Interpretation

Magnetic survey is very helpful in identifying geological structures and contact zones of different lithologies. Therefore, the corrected data is then processed using different software and different maps and model were produced like magnetic anomaly map, analytical signal map and 2D magnetic model.

5.2.1 Magnetic anomaly map

The raw magnetic data were corrected for diurnal variation. The magnetic anomaly was determined after reducing the IGRF values that determined in the area. The data that is produced from the corrected magnetic data is given with the magnetic anomaly map of the survey area as shown in Figure 5.6. From the magnetic anomaly map, the subsurface condition shows that high and low magnetic response corresponding to the presence of high and low magnetic materials. The high magnetic anomaly response is probably due to the result of massif basalt rock and covers more in the northeastern and some in central part of the study area.

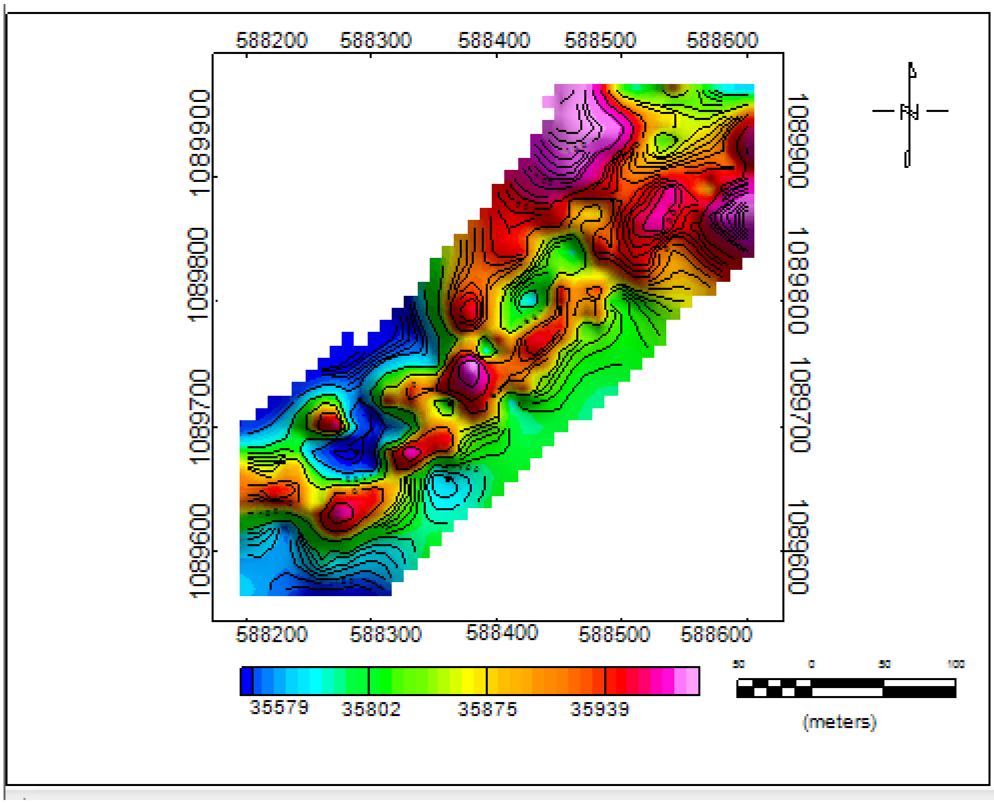

Figure 5.6 Magnetic anomaly map of the study area.

The intermediate and low magnetic anomalies zones may be the response of jointed, fractured and weathered basalt and ignimbrite rocks and the overlain colluvial deposits as well. It covers almost the northeastern and central parts of the survey area.

5.2.2 Analytical signal map

From the magnetic data it was possible to construct an analytical signal map shown in Figure 5.7. The map shows the responses of anomalous bodies just from the upper part of their sources. The analytic signal map is well resolved for shallow anomaly sources but may not be as such well resolved for deep sources and is good at locating the edges of shallow bodies. The amplitude of the simple analytical signal peaks (maxima) over magnetic contacts does not depend on the directions (inclinations) of magnetization. In addition to these, the map shows zones within the survey area associated with geological contacts. This analytical map shows that the anomalous bodies are in southwestern part of the survey area.

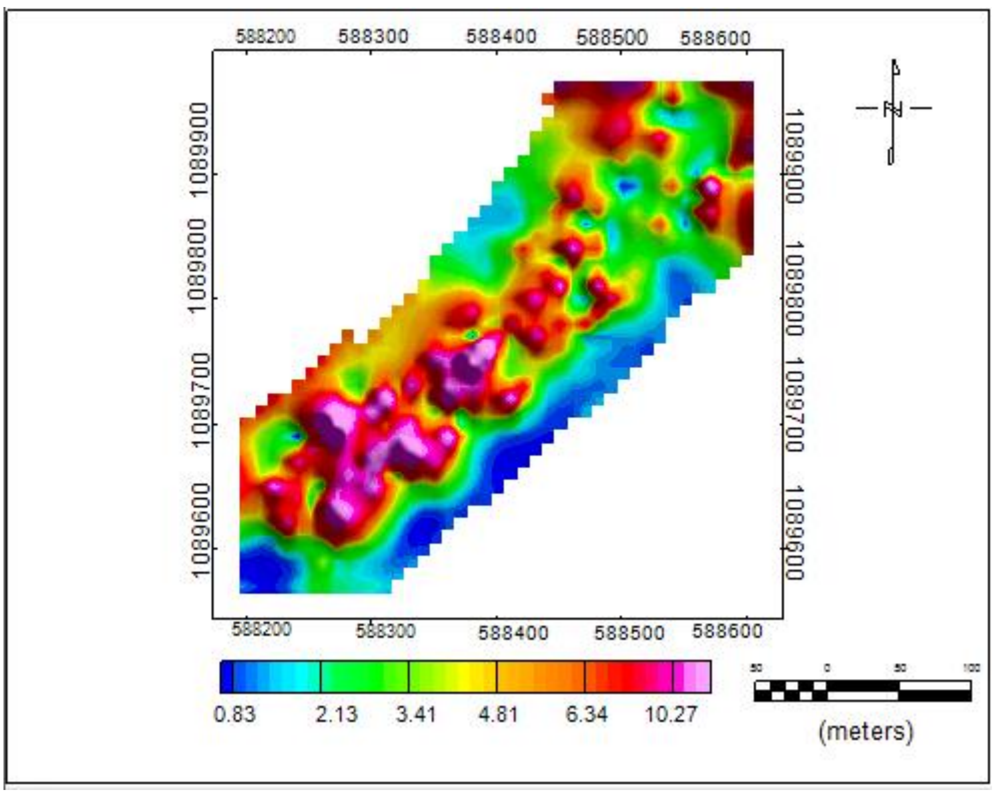

Figure 5.7 Analytical signal map of the study area.

5.2.3 Horizontal gradient map

This map is important for edges detection of magnetic causative bodies. It is also important to enhance lithological changes, structural regimes, deformation styles and trends. The horizontal gradient map of the study area was developed by 45^{o} gradient direction which is counter clockwise from +X axis. The map shows that the location of two fracture zones in the center and northeastern part of the survey area.

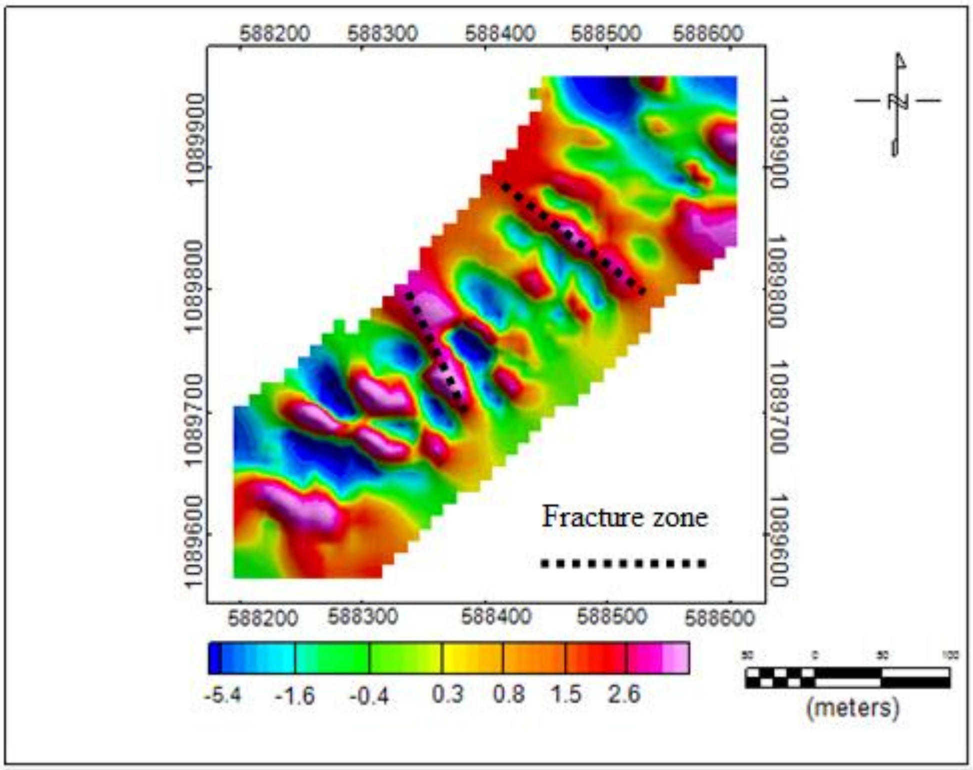

Figure 5.8 Horizontal gradient map

5.2.4 Magnetic 2D-Model

The 2D-magnetic model was developed using GM-SYS component of the Oasis Montaj 6.4.2 software. It is also constrained by the magnetic susceptibility and depths of the geological lithologies in the study area. This model helps to see the subsurface variations of lithologies, geological contacts and structures.

The model shows the location of geological structures at the southwest and near to northeast direction of the geophysical surveyed site. The model was done at profile-3 just down the road and clearly indicates that the thickness of the highly weathered basalt rock is high just down the road.

This is also significant input for sliding problem of the main asphalt road at the southwest and northeast direction of the profiles.

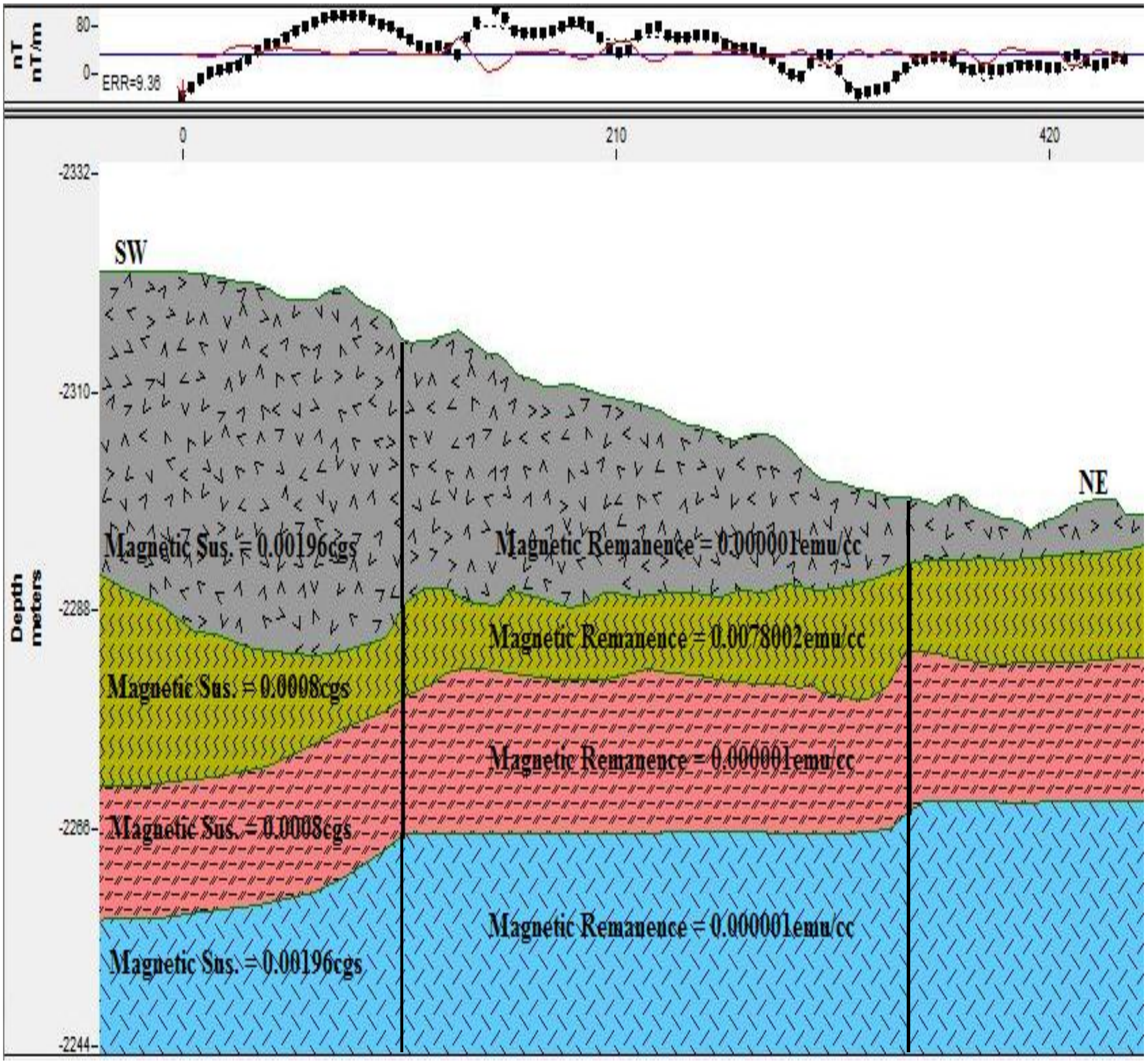

Figure 5.9 Magnetic model of profile-3

LEGEND

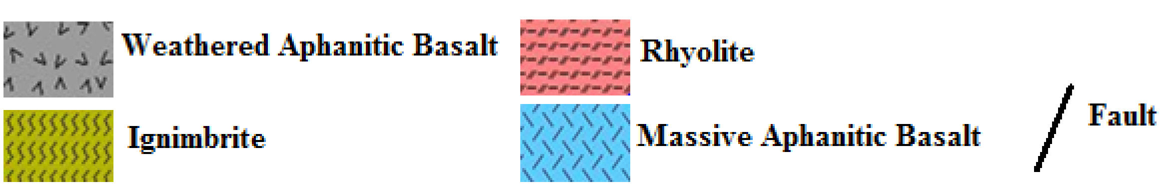

CHAPTER - SIX

CONCLUSION AND RECOMMENDATION

6.1 Conclusions

Geophysical and geological investigations have been conducted for landslide problem characterization of the existing main road of the study area. The purpose of this research was to provide an understanding of the subsurface processes and extents of landslide on a major asphalt road of the study area by means of geophysical techniques with the target of reducing landslide risk to lives and infrastructures. Due to the significant contrasts between the physical properties of the disturbed and undisturbed mass, the results from the geophysical techniques have clearly outlined valuable information's about the subsurface conditions and possible processes of the landslide affected road section.

ERT data modelling was also performed with the topography information of the study area to indicate the undulated and sloped nature of the area. The image indicates that the cause of sliding problem in the area which was due to its sloped topography and the associated weak zones. The interpretation of ERT data shows that there is a possible occurrence of landslide at all northeast and southwest direction of the survey profiles of the area.

Based on the combined interpretations, the subsurface condition of the main asphalt road is in highly disturbed and fragmented zones. Moreover, the clay soil is dominant at northeast direction of the area in the whole three profiles. Particularly, profile three indicates huge subsurface depth of the road is covered totally by fragmented and residual sediments which are suitable for sliding happenings in the area particularly northeast and southwest end of the survey area.

Therefore, northeastern side of the main asphalt road of the survey area needs special care and speedy remedial measures because all the result of the study indicate the possible sliding surface is in the northeastern side of the surveyed area and this is also confirmed through field observations.

The magnetic profiles remarkably coincide with the 2D electrical resistivity profiles in mapping the weak zones. The high magnetic anomaly response is probably due to the result of highly magnetized volcanic rocks that could be found in the area. The higher the magnetic response the shallower the fresh volcanic rocks are believed to be the bedrocks in the area. The intermediate and low magnetic anomalies are the responses of different degree of fracturing of the volcanic rocks and regions around the weak zones.

The occurrences of springs and seepages have significant influence on the initiations of landslide problem. Finally, the main triggering factors for landslide problem in the area have clearly outlined. These are intense weathered condition of the geological lithologies and geological structures, sloped morphology, high rainfall conditions and seismicity of the area.

6.2 Recommendations

Based on the outcomes of this research, the following recommendations are made in relation to the land sliding problem in the main asphalt road of the area:

- The geophysical investigations have revealed that sub-surface conditions of the road are highly susceptible to active landslide which may have adverse effect on the existing road. Therefore, it is strongly recommended that concerned organizations take appropriate remedial measures on the slope and drainage system of asphalt road.
- The main road is highly affected by landslide problem, especially from Shola Meda up to Armania town; moreover, the geophysical results indicate that the subsurface condition of the main road has significant thickness of clay soils, fracturing basalt rocks and weak zones to the direction of northeast of study area. Therefore, it needs special remedial measures and prevention techniques form future sliding problems.
- From field observations, occurrence of groundwater, springs and seepages have important role for sliding problem of the road and the whole study area, especially in the rainy season they increase in number and discharge rate in all sloped area of study. Therefore, proper control of external and internal drainage system of the road is required.
- The current study covered only one section of the main road but the problem is in the whole Addis Ababa- Dessie- Mekelle main road. So, to prevent all types of economic losses and inhibiting traffics from this landslide problem, additional detailed and comprehensive investigation will be required for the whole main asphalt road.
- Because of the financial problem and shortage of time the current study was limited to 2D-Electrical Imaging, Magnetic and Geological investigations part only. So, it will be good for future researchers to include Seismic refraction and geotechnical investigations.

REFERENCES

Alula, H. and Gashawbeza, M., 1993. Report on coal occurrence of Mush Valley. EIGS, Addis Ababa.

Asmelash A., (2012). Remote Sensing & GIS-based Mapping on Landslide Phenomena & Landslide Susceptibility Evaluation of Debresina area, Ethiopia: PhD Thesis. Università degli Studi di Cagliari.

Asmelash A., Giulio B., (2012). Investigation of landslide susceptibility and causative factors evaluation of the landslide area of Debresina, in the Southwestern Afar Escarpment, Ethiopia: Journal of Earth Science and Engineering 2, 133-144.

Ayalew L., (1999).The effect of seasonal rainfall on landslides in the highlands of Ethiopia, Bull Eng Geol Env. 58: 9-19, Q Springer-Verlag.

Ayalew L., Yamagishi H., (2004).Slope movements in the Blue Nile basin, as seen from landscape evolution perspective. Geomorphology, 57:97-116.

Ayenew T., Barbieri G., (2005).Inventory of landslides and susceptibility mapping in the Dessie area. Northern Ethiopia, Eng. Geology 77:1-15.

Blakely R.J. (1995), Potential theory in Gravity and Magnetic applications. Cambridge University Press, Australia. pp 461.

DeGroot-Hedlin, C. and Constable, S. (1990). Occam's inversion to generate smooth, two dimensional models form magneto telluric data. Geophysics, v 55, 1613-1624.

EIGS, 1994. Engineering geophysical investigation along proposed alternative route, Blue Nile Gorge. EIGS. Ethiopia. Unpublished report.

EIGS, 1999. Integrated engineering geological and geophysical investigation for Landslides study in Bonga town and its surrounding. EIGS. Ethiopia. Unpublished report.

Ethiopian Building Code Standard (1995). Code of Standards for Seismic Loads. Ministry of Works and Urban Development, Addis Ababa, Ethiopia.

Getech (2007). Advanced Processing and Interpretation of Gravity and Magnetic Data (available at http: //www.getech.com).

Griffiths, D.H. and Barker, R.D. (1993). Two-dimensional resistivity imaging and modelling in areas of complex geology, Applied Geophysics, v 29, 211-226.

Kearey. P. Brooks. M. and Hill. I., (2002). An Introduction to Geophysical Exploration, 3rd ed., Blackwell Science Ltd., pp 160.

Kirsch, R. (2009). Groundwater Geophysics. 2nd Edition. Hamburger Chaussee, Germany, p 275-286.

Leta A., (2007). Landslide Susceptibility Modeling Using Logistic Regression and Artificial Neural networks in GIS: a case study in Northern Showa area, Ethiopia. MSc Thesis, Addis Ababa university earth science department: 75pp.

Loke, M.H. (1999). Electrical imaging surveys for environmental and engineering studies. A Practical guide to 2-D and 3-D surveys, Penang, Malaysia, pp 67.

Lowrie, W. (2007). Fundamentals of Geophysics. 2nd Edition. Cambridge University, p 326.

McDowell, P .W, Dr Barker, R. D, Butcher, A.P, Dr Jackson P.D, Pro. McCann, D.M and Dr Sdipp, B.O (2002). Geophysics in Engineering Investigation. 6 Storey's Gate, Westminster, London, pp 249.

Mengesha T., Tadiwos C. & Workineh H., (1996). Explanation of the Geological Map of Ethiopia, Scale 1:2,000,000, 2nd edition. Addis Ababa: The Federal Democratic Republic of Ethiopia.

Milson, J. (2003). Field Geophysics. 3rd Edition. University College London, pp 249.

Reilly (1972). Use of International System of Units in Geophysical Publications. N. Z. J. Geol. Geophysics, 15, 148-58.

Reynolds, J.M. (1997). An Introduction to Applied and Environmental Geophysics. John Wiley and Sons limited, England, UK. p 116-209, 415-522.

Rivas, J.E. (2009). Geothermal training programme: gravity and magnetic methods Ahuachapán and Santa Tecla, El Salvador, United Nations University, pp 13.

Roest, W.R., Verhof, J. Pilkington, M. (1992). Magnetic interpretation using 3D analytic signal. Geophysics, 57, 116-125.

Salem, A., Ravat, D., Gamey, T. J. and Ushijuma, K. (2002). Analytic signal approach and its applicability in environmental magnetic investigation. Journal of Appl. Geophysics, 49; 231-244.

Singh, S.K. (1997). Dynamic deformation of shallow sediments in the valley of Mexico, part II: Single station estimates. Bull. Seismol. Am. v 87, 540-550.

Solomon G. (2010). Integrated landslide investigations in Tarmaber and surroundings, north Shewa zone, Amhara regional state. EGS, Ethiopia. Unpublished report.

Temesgen B., Mohammed M.U., Korme T., (2001).Natural hazard assessment using GIS and remote sensing methods, with particular reference to the landslides in the Wondogenet area, Ethiopia. Phys. Chem. Earth., 26 (9):665-675.

Thomas, M.B. (2003). Introduction to geophysical exploration: magnetic notes on main magnetic field (available at galitzin.mines.edu/…/notes).

Tigistu Haile (2010). Applications of electrical resistivity tomography (at www.mawari.net.). pp 6.

Woldearegay K., (2005). Rainfall-triggered landslides in the northern highlands of Ethiopia: Characterization, GIS-based Prediction and Mitigation. PhD Thesis. Facul. of Civil Eng. Graz Univ. of Techno. 176pp.

Yonas H. and Matebie M., 2006. Geology of Sela Dingay(C) and Debre Berhan (J) sub sheets of Debre Berhan map sheet. GSE, Addis Ababa, Ethiopia.

Zanettin, B. & Justin Visentin, E., (1974).The volcanic succession in central Ethiopia, 2: The volcanics of the western Afar and Ethiopia rift margins.Memorie degli Istituti di Geologia e Mineralogia dell"Universita di Padova 31: 1-19.

Annex-I: Average, maximum and minimum monthly rainfalls of Debresina Metrological station for last 33 years (1980-2012).

MONTH	AVER	MAX	MIN
JAN	67.35152	235.4	0
FEB	47.58485	149.8	0
MAR	127.6182	415.2	0.5
APR	157.1212	401.1	20.8
MAY	124.6152	437.6	4
JUN	71.48485	225.5	0
JUL	368.6273	675.3	27.7
AUG	432.6455	727.2	97
SEP	185.5424	454.6	21.1
OCT	81.29643	271.7	0
NOV	54.84349	245.9	0
DEC	69.18485	327.4	0

Annex-II: Resistivity of some common rocks is given in (Loke, 1999).

Material	**Resistivity (Ωm)**	**Conductivity (Siemen/m)**
Igneous and Metamorphic Rocks		
Granit	5×10^{3} - 10^{6}	10^{-6} – 2×10^{-4}
Basalt	10^{3} – 10^{6}	10^{-6} -10^{-3}
Slate	610^{2} – 4×10^{7}	2.5×10^{-8} – 1.7×10^{-3}
Marble	10^{2} – 2.5×10^{8}	4×10^{-9} – 10^{-2}
Quartzite	10^{2} - 2×10^{8}	5×10^{-9} – 10^{-2}
Sedimentary Rocks		
Sandstone	8 -4×10^{3}	2.5×10^{-4} – 0.125
Shale	20 -2×10^{3}	5×10^{-4} – 0.05
Limestone	50 - 4×10^{2}	2.5×10^{-3} – 0.02

Annex-III: Magnetic susceptibilities and resistivities of some common rocks, soils water and minerals (Milson, 2003)

Mineral or rock types	Susceptibility (k) (rationalized SI units)	Mineral or rock types	Resistivity (ohm- m)
Dolomite (pure)	-12.5 to 44	Igneous and Metamorphic Rocks	
Dolomite (impure)	20,000	Granite	$5x10^3$-10^6
Limestone	10 to 25,000	Basalt	10^3-10^6
Sandstone	0 to 21,000	Slate	$6x10^2$-$4x10^7$
Shale	60 to 18,600	Marble	10^2-$2.5x10^8$
Schist	315 to 3000	Quartzite	10^2-$2x10^8$
Slate	0 to 38,000	Sedimentary Rocks	
Gneiss	125 to 25,000	Sandstone	8-$4x10^3$
Serpentenite	3,100 to 75,000	Shale	20-$2x10^3$
Granite	20 to 50,000	Limestone	50-$4x10^2$
Rhyolites	250 to 37,7000	Soils and waters	
Pegmatite	3,000 to 75,000	Clay	1-1000
Gabbro	800 to 76,000	Alluvium	10-800
Basalts	5000 to 182,000	Groundwater (fresh)	10-100
Oceanic Basalts	300 to 3,6000	Sea water	0.2
Perdotite	95,000 to 196,000		

Annex-IV: Photographs showing landslide effects on the main road, electrical tower and local house of study area.

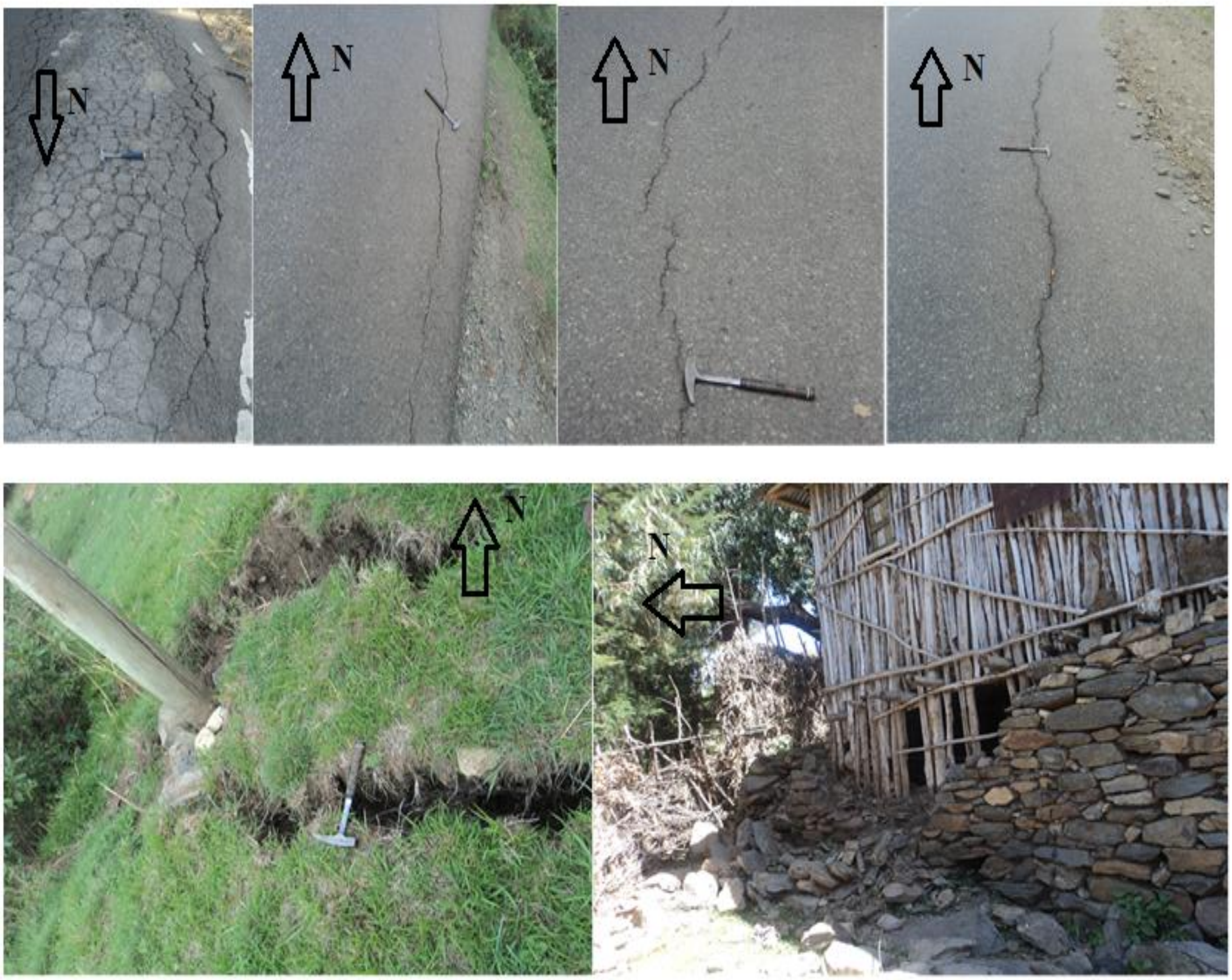
N
N
N
N
N
N